COMILLAS
UNIVERSIDAD PONTIFICIA
ICAI

OFFICIAL MASTER IN INDUSTRIAL ENGINEERING

MASTER THESIS DISSERTATION

SPALLING BEHAVIOUR OF CONCRETE IN FIRE: EFFECT OF DIFFERENT FIBERS

Author: Marta Tena Briceño

Supervisor: Dr. Alberto Carnicero López

Deputy Supervisor: Dr. Alexis Cantizano González

Madrid

July 2019

To my parents, my friends and my teachers

AUTORIZACIÓN PARA LA DIGITALIZACIÓN, DEPÓSITO Y DIVULGACIÓN EN RED DE PROYECTOS FIN DE GRADO, FIN DE MÁSTER, TESINAS O MEMORIAS DE BACHILLERATO

1º. Declaración de la autoría y acreditación de la misma.
El autor D. Marta Tena Briceño_____

DECLARA ser el titular de los derechos de propiedad intelectual de la obra: SPALLING BEHAVIOUR OF CONCRETE IN FIRE: EFFECT OF DIFFERENT FIBRES, que ésta es una obra original, y que ostenta la condición de autor en el sentido que otorga la Ley de Propiedad Intelectual.

2º. Objeto y fines de la cesión.
Con el fin de dar la máxima difusión a la obra citada a través del Repositorio institucional de la Universidad, el autor **CEDE** a la Universidad Pontificia Comillas, de forma gratuita y no exclusiva, por el máximo plazo legal y con ámbito universal, los derechos de digitalización, de archivo, de reproducción, de distribución y de comunicación pública, incluido el derecho de puesta a disposición electrónica, tal y como se describen en la Ley de Propiedad Intelectual. El derecho de transformación se cede a los únicos efectos de lo dispuesto en la letra a) del apartado siguiente.

3º. Condiciones de la cesión y acceso
Sin perjuicio de la titularidad de la obra, que sigue correspondiendo a su autor, la cesión de derechos contemplada en esta licencia habilita para:

a) Transformarla con el fin de adaptarla a cualquier tecnología que permita incorporarla a internet y hacerla accesible; incorporar metadatos para realizar el registro de la obra e incorporar "marcas de agua" o cualquier otro sistema de seguridad o de protección.
b) Reproducirla en un soporte digital para su incorporación a una base de datos electrónica, incluyendo el derecho de reproducir y almacenar la obra en servidores, a los efectos de garantizar su seguridad, conservación y preservar el formato.
c) Comunicarla, por defecto, a través de un archivo institucional abierto, accesible de modo libre y gratuito a través de internet.
d) Cualquier otra forma de acceso (restringido, embargado, cerrado) deberá solicitarse expresamente y obedecer a causas justificadas.
e) Asignar por defecto a estos trabajos una licencia Creative Commons.
f) Asignar por defecto a estos trabajos un HANDLE (URL *persistente)*.

4º. Derechos del autor.
El autor, en tanto que titular de una obra tiene derecho a:

a) Que la Universidad identifique claramente su nombre como autor de la misma
b) Comunicar y dar publicidad a la obra en la versión que ceda y en otras posteriores a través de cualquier medio.
c) Solicitar la retirada de la obra del repositorio por causa justificada.
d) Recibir notificación fehaciente de cualquier reclamación que puedan formular terceras personas en relación con la obra y, en particular, de reclamaciones relativas a los derechos de propiedad intelectual sobre ella.

5º. Deberes del autor.
El autor se compromete a:

a) Garantizar que el compromiso que adquiere mediante el presente escrito no infringe ningún derecho de terceros, ya sean de propiedad industrial, intelectual o cualquier otro.
b) Garantizar que el contenido de las obras no atenta contra los derechos al honor, a la intimidad y a la imagen de terceros.
c) Asumir toda reclamación o responsabilidad, incluyendo las indemnizaciones por daños, que

pudieran ejercitarse contra la Universidad por terceros que vieran infringidos sus derechos e intereses a causa de la cesión.

d) Asumir la responsabilidad en el caso de que las instituciones fueran condenadas por infracción de derechos derivada de las obras objeto de la cesión.

6º. Fines y funcionamiento del Repositorio Institucional.

La obra se pondrá a disposición de los usuarios para que hagan de ella un uso justo y respetuoso con los derechos del autor, según lo permitido por la legislación aplicable, y con fines de estudio, investigación, o cualquier otro fin lícito. Con dicha finalidad, la Universidad asume los siguientes deberes y se reserva las siguientes facultades:

- La Universidad informará a los usuarios del archivo sobre los usos permitidos, y no garantiza ni asume responsabilidad alguna por otras formas en que los usuarios hagan un uso posterior de las obras no conforme con la legislación vigente. El uso posterior, más allá de la copia privada, requerirá que se cite la fuente y se reconozca la autoría, que no se obtenga beneficio comercial, y que no se realicen obras derivadas.
- La Universidad no revisará el contenido de las obras, que en todo caso permanecerá bajo la responsabilidad exclusive del autor y no estará obligada a ejercitar acciones legales en nombre del autor en el supuesto de infracciones a derechos de propiedad intelectual derivados del depósito y archivo de las obras. El autor renuncia a cualquier reclamación frente a la Universidad por las formas no ajustadas a la legislación vigente en que los usuarios hagan uso de las obras.
- La Universidad adoptará las medidas necesarias para la preservación de la obra en un futuro.
- La Universidad se reserva la facultad de retirar la obra, previa notificación al autor, en supuestos suficientemente justificados, o en caso de reclamaciones de terceros.

Madrid, a 3 de julio de 2019

ACEPTA

Fdo 

Motivos para solicitar el acceso restringido, cerrado o embargado del trabajo en el Repositorio Institucional:

COMILLAS
UNIVERSIDAD PONTIFICIA
ICAI

OFFICIAL MASTER IN INDUSTRIAL ENGINEERING

MASTER THESIS DISSERTATION

SPALLING BEHAVIOUR OF CONCRETE IN FIRE: EFFECT OF DIFFERENT FIBERS

Author: Marta Tena Briceño

Supervisor: Dr. Alberto Carnicero López

Deputy Supervisor: Dr. Alexis Cantizano González

Madrid

July 2019

Declaro, bajo mi responsabilidad, que el Proyecto presentado con el título

Spalling behaviour of concrete in fire: effect of different fibers

en la ETS de Ingeniería - ICAI de la Universidad Pontificia Comillas en el curso académico 2018/2019 es de mi autoría, original e inédito y no ha sido presentado con anterioridad a otros efectos. El Proyecto no es plagio de otro, ni total ni parcialmente y la información que ha sido tomada de otros documentos está debidamente referenciada.

Fdo.: Marta Tena Briceño Fecha: 3/07/2019

Autorizada la entrega del proyecto

EL DIRECTOR DEL PROYECTO

Fdo.: Alberto Carnicero López y Alexis Cantizano

Fecha: ……/ ……/ ……

Firmado digitalmente por carnicero@comillas.edu
Nombre de reconocimiento (DN): cn=carnicero@comillas.edu
Fecha: 2019.07.08 16:45:06 +02'00'

Firmado digitalmente por alexis.cantizano@comillas.edu
Nombre de reconocimiento (DN): cn=alexis.cantizano@comillas.edu
Fecha: 2019.07.08 17:12:34 +02'00'

Contents

Abstract **xiii**

Resumen **xv**

1. Introduction **1**
1.1. The field . . . 1
1.2. Motivation . . . 2
1.3. Objective . . . 2
1.4. Project Objectives . . . 3
1.5. Methodology . . . 3

2. State of the Art **5**
2.1. Introduction . . . 5
2.2. Eurocode . . . 5
2.3. Previous Concrete Spalling Studies . . . 8
2.4. Theoretical Studies . . . 15
2.5. Describing Spalling . . . 17
2.5.1. Thermo-hydrauluc mechanisms . . . 17
2.5.2. Thermo-mechanical mechanisms . . . 17
2.5.3. Thermo-chemical mechanisms . . . 17
2.6. Quantification of the appearance of spalling . . . 18
2.7. Parameters influencing spalling . . . 19
2.7.1. Moisture content . . . 21
2.7.2. Aggregates . . . 21
2.7.3. Curing . . . 22
2.7.4. Compressive Stress and compressive strength . . . 22
2.7.5. Water to Cement Ratio . . . 23
2.7.6. Age of Specimen . . . 24
2.7.7. Heating Techniques . . . 24
2.7.8. Mechanical Load . . . 25
2.7.9. Density . . . 26
2.7.10 Permeability . . . 27
2.7.11 Silica fume . . . 27
2.7.12 Pore pressure . . . 27
2.7.13 Fibers . . . 28
2.7.14 Outcome . . . 28
2.8. Types of Spalling . . . 29
2.9. Conclusions . . . 30

3. Experimentation **31**
3.1. Exposing concrete samples to high temperatures . . . 31
3.2. Cores . . . 32
3.3. Decoloration . . . 38
4. Compression and Tension Testing **43**
4.1. Compression and Tension Testing . . . 43
4.2. Compression . . . 44
4.3. Tension . . . 46
5. Finite Element Simulations **49**
5.1. Introduction . . . 49
5.2. Thermal Model . . . 49
5.3. Conclusions . . . 52
6. Numerical Model with Matlab **55**
6.1. Introduction . . . 55
6.2. Reproducing plain concrete . . . 56
6.2.1. PDE Model . . . 56
6.2.1.1. Geometry . . . 56
6.2.1.2. Mesh . . . 57
6.2.1.3. Boundary Conditions . . . 58
6.2.2. Thermal model verification . . . 59
6.2.3. Transient Thermal . . . 59
6.2.4. Moisture . . . 60
6.2.5. Thermal with moisture disengaged . . . 60
6.2.6. Conclusion . . . 62
7. Conclusion **63**
7.0.1. Future . . . 64
8. Annex **65**
8.1. Thermal Model Verification Code . . . 66
8.2. Transitient thermal Code . . . 68
8.3. Moisture Code . . . 70
8.4. Thermal with moisture disengaged Code . . . 72
Bibliografía **74**
Bibliography **75**

List of Figures

Figure 2.1. Relation between temperature and density by Eurocode 6
Figure 2.2. Specific heat of concrete by Eurocode 6
Figure 2.3. Conductivity of concrete by Eurocode 6
Figure 2.4. Elastic Modulus of concrete with increasing temperature 7
Figure 2.5. Variation of compressive strength of concrete by Eurocode 7
Figure 2.6. Variation of tensile strength of concrete by Eurocode 8
Figure 2.7. Thermal expansion of concrete by aggregate concrete by Eurocode 8
Figure 2.8. Meller-Ottens 1965, Heat exposure and risk of spalling 9
Figure 2.9. Zhukoc 1975, Spalling relation with moisture content 9
Figure 2.10. Rilem workshop table 1. 12
Figure 2.11. Rilem workshop table 2. 13
Figure 2.12. Rilem workshop table 3. 14
Figure 2.13. Moisture clog formation by Harmathy. 15
Figure 2.14. Dougill 1971, explanation of stress action on spall 16
Figure 2.15. Categorization of factor which affect spalling 17
Figure 2.16. Variables which affect spalling quantified by Arup Fire 2005 18
Figure 2.17. Arup Fire 2005, Spalling categories. 19
Figure 2.18. Relationship between spalling parameters 20
Figure 2.19. Depth of spalling with different concrete aggregates 21
Figure 2.20. Depth of spalling when aggregate has different sizes 22
Figure 2.21. Spalling when cured in different conditions by Izabela Hager and Tomas Zdeb 22
Figure 2.22. Variation of compressive strength with temperature by Metin Husem 23
Figure 2.23. Spalling mass and damage level by Marcus Maier and Roman Lackner . . . 23
Figure 2.24. Spalling start time and duration by Marcus Maier and Roman Lackner . . . 24
Figure 2.25. Temperature of the spall related to the heating rate 25
Figure 2.26. Effect of the load applied in the spalling time 26
Figure 2.27. Variation of mass with rising temperature, Kodur 2012 26
Figure 2.28. Temperature influence in permeability of concrete 27
Figure 2.29. Temperature influence in concrete porosity, Bazant and Kaplan (1996) . . . 27
Figure 2.30. Types of spalling defines by Dougill, 1971 29
Figure 2.31. Critical spalling temperatures defined before 29
Figure 3.1. Location of the thermo-couples from the exposed surface. 32
Figure 3.2. Position of the blocks extracted from each block. 32
Figure 3.3. Maximum temperature of each thermocouple in mix 1A.. 38
Figure 3.4. Maximum temperature of each thermocouple in mix 1B.. 38

Figure 3.5. MMaximumax temperature of each thermocouple in mix 2A.. 39
Figure 3.6. Maximum temperature of each thermocouple in mix 2B.. 39
Figure 3.7. Maximum temperature of each thermocouple in mix 3A.. 39
Figure 3.8. Maximum temperature of each thermocouple in mix 3B.. 39
Figure 3.9. Maximum temperature of each thermocouple in mix 4A.. 39
Figure 3.10. Maximum temperature of each thermocouple in mix 4B.. 40
Figure 3.11. Maximum temperature of each thermocouple in mix 5A.. 40
Figure 3.12. Maximum temperature of each thermocouple in mix 5B.. 40
Figure 3.13. Maximum temperature of each thermocouple in mix 6A.. 40
Figure 3.14. Maximum temperature of each thermocouple in mix 6B.. 41
Figure 4.1. Lawyers extracted from each core. 43
Figure 4.2. Correction factor depending on the L/D relation.. 44
Figure 4.3. Plot of the compression strength for the back (blue) and middle (red) lawyers.. 45
Figure 4.4. Plot of the Max (red) and min (blue) temperatures of each sample.. 45
Figure 4.5. Example of a Brazilian test from one of the samples. 46
Figure 4.6. Plot of the tensile strength for the back (blue) and middle (red) layers. . . . 47
Figure 5.1. Mesh developed for the Ansys model 50
Figure 5.2. Heat flux data imported to the model from the experiment in The University of Queensland 50
Figure 5.3. Temperature distribution resulting of the ansys simulation 51
Figure 5.4. Temperature distribution through time graph resulting of the ansys simulation 51
Figure 5.5. Recorded temperature in the thermo-couples of plain concrete when exposed to the heat flux 52
Figure 5.6. Graph of the recorded temperature in the thermo-couples of plain concrete when exposed to the heat flux 52
Figure 6.1. Geometry to be studied 57
Figure 6.2. Mesh created 57
Figure 6.3. Temperature obtained by the heat flux generated in The University of Queensland 58
Figure 6.4. Matlab results for a transient Thermal with constant coefficients,heat flux . 59
Figure 6.5. Matlab results for a transient Thermal 60
Figure 6.6. Matlab results for a transitient Thermal 60
Figure 6.7. Matlab results for a 2 PDE model with a unique boundary condition 61
Figure 6.8. Matlab results for a 2 PDE model with a 3 boundary condition 62

Abstract

Building construction is something that has taken part in humanity since its origins. The necessity to find a place to sleep, feel safe, a place where we can find confort with our significants, is something present in our DNA.

Through out history construction has been characterized for the use of different materials. As society moved on, materials did so with it. The discovery and experimentation of different materials has been key to be able to come where we are today.
Concrete is currently, the most used material in construction. It is a material originated with the mixture of many others such as: water, cement, aggregates, mostly; but many others too. The combination and different quantities of each component determine the mechanical properties of the material, hence concrete can not be charadtericed with constant properties.

To improve this material, during the years, many fibers have been introduced so that the properties developed with it depending on the application wanted.

Concrete is considered a material resistant to fire. Although, this is not fully true. Recent events such as Liverpool Echo Arena fire and Grenfell Tower fire have made it clear that it is not a material keen for high temperatures, due to the uncapability to stay in one piece. This is due to the appearance of the phenomenon spalling. This phenomenon originates when high temperatures are reached, this make water in the interior of concrete to evaporate and the following search for a way out. This way out is normally something unavoidable and it forces the material to crack out due to the lack of places to go.

The first part of this thesis gathers the study of concrete with different fibers (different materials: plastic, polypropylene, steel). In case of plastic the fibers melt letting the vapour out through out the channels created. Steel fibers do not guarantee the melting of the material (higher temperatures should be reached) yet the strength of the material helps concrete stay together even if it cracks.

The second part of the thesis, consists on the analysis of all the previous works on spalling both theoretical and experimental since 1900. The analysis of the parameters that affect this phenomenon and how this interactuate with each other.

The third and final part of the project gathers the elaboration of a program that simulates the occurrence of the spalling event. The experiment of different softwares such as ansys and matlab and the elaboration of this code.

Key words: Spalling · Concrete · fire · simulation ·

Resumen

La construccion es algo que ha formado parte en la humanidad desde los orígenes del hombre. La necesidad de encontrar un lugar donde refugiarnos, sentirnos seguros, donde poder ir a estar con los nuestros ha sido algo presente en nuestro ADN.

A lo largo de la historia diferentes materiales han sido usados para la construccion. Conforme la sociedad avanzaba, los materiales evolucionaban. El descubrimiento y experimentacion de diferentes materiales ha sido clave para llegar a donde estamos ahora.
El concreto es el material más usado en la construcción actualmente. Es un material originado por la mezcla de varios materiales: agregados, agua y cemento, en mayor parte. La combinación y distintas cantidades de cada componente determinan las propiedades mecánicas del material, por eso es que no se podría cualificar como únicas las propiedades mecánicas del hormigón.

Para mejorar este material durante los años se han ido introduciendo diferentes fibras de tal forma que mejoran las propiedades dependiendo de la aplicación que se quiera para este.

El hormigón es considerado un material con gran resistencia al fuego. Sin embargo, esto no es del todo cierto. Los eventos recientes como en el "Liverpool echo arena.º la torre de Grenfell han demostrado que es un material que a altas temperaturas tiene dificultades para mantenerse de una pieza.

Esto es debido a la aparición de un fenómeno denominado "spalling", palometeo en castellano. Este fenomeno surge cuando altas temperaturas son alcanzadas, lo que hace que el agua dentro del hormigón se evapore y busqué salir . Ese camino hacia el exterior suele ser forzoso debido a la falta de lugares por los que escapar.

En la primera parte de esta tesis, se recoge el estudio de diferentes hormigones con fibras de distintos materiales en su interior. Estas fibras, pudiendo ser de plástico o de acero, en el caso de plastico se derriten a estas altas temperaturas dejando así un canal por el cual podría escapar el vapor. Con las de acero no se produce ese derretimiento, sin embargo debido a su fuerza es capaz de sujetar mejor el hormigón a pesar de la fuerza ejercida por el vapor para salir.

La segunda parte de la tesis, consiste en el anaisis de todos los trabajos realizados desde 1900 sobre este tema, analisis de los parametros que afectan a este fenómeno y cómo interactúan entre sí.

La tercera parte del proyecto recoge la elaboración de un programa que simule la aparicion de este fenómeno denóminado palometeo. Así es que este documento recoge la experiencia con diferentes softwares utilizados y como se ha ido elaborando ese programa.

Palabras clave: Palometeo · Hormigón · fuego · simulación

1 Introduction

This first chapter introduces the rationale behind this thesis as well as its main objectives. In addition, it provides the reader with a general overview of the organization and the outline of the dissertation in order to make it easier to follow.

1.1. The field

The field of construction has made it possible for humans to develop as a special species throughout time. It made our ancestors move from caves to the making of civilizations. In the beginning the materials used were simple ones: mud and clay both with the aid of straws, hay, sticks; mainly organic materials. The main use for these additives was for the improvement of the mechanical properties of the whole construction. As civilization developed these materials developed with it. Wood, ticks, large piles of rocks were the following materials used as people observed that the mechanical properties were better.

The main improvement was when civilization produced composite materials such as concrete and cement. This resulted on a big change due to the building materials were not raw but the outcome of research and human manipulation. These elaborated composites differ depending on the compound materials, the proportions and different aggregates.

Now-a-days glass, metal (such as steel) are important materials for making buildings more practical, resistant, and aesthetically pretty which is a new characteristic. This has appeared in contrast with previous eras, due to the decrease in the need of protection and the increase of human capability to produce new things. Since metal and glass result sensitive to corrosion and lack endurement it was logical for the civilization to develop new materials whose characteristics enhance those of the predecessors. These materials are plastics such as polymers. The improvement of the features and the lightweight and the ease of molding plastic made it easy to use these material.

The addition of these new materials has not displaced conventional ones such as concrete. Concrete is the most important material in building construction used in buildings, bridges, roads and all sort of projects. It is a composite material consisting of mostly cement, water

and aggregate. The portions of these materials as well as the type of aggregate give concrete different mechanical characteristics and make it very versatile to work with.

The benefits of concrete are:

- versatile
- cheap
- lasting
- few maintenance requirements
- strong with compression
- easily shaped
- non-combustible

The limitations of concrete are:

- low tensile strength
- low ductility
- low stregth-to-weight ratio
- few maintenance requirements
- susceptible to cracking

1.2. Motivation

In the previous years, catastrophes have occurred in several concrete buildings due to fire. Two significant fires have taken place such as the Grenfell Tower fire (14 June 2017) and the Liverpool Echo Arena car park fire (31 December 2017). In both fires, the structures did not collapse even though an extensive phenomenon of spalling (an explosive loss of the surface material) occurred. Although rare, catastrophic fires as these two can have severe and dramatic economic and safety consequences. Concrete is a material susceptible to spalling and spalling is a phenomenon not very well known and not well understood there for the need of research to comprehend it.

Fires like these can happen anywhere in the world at any time that is why we need to study the materials to make them as safe as possible for the prevention of catastrophes.

My motivation due to the need described and how with my work we can make the world a little safer.

1.3. Objective

The main objective of the project is to understand the spalling behavior and all the characteristics taking place in the process, also, try to reproduce the spalling effect in concrete samples under fire exposure, hence understanding this complex phenomenon. Since this event is not yet fully understood it is of high importance to understand the experiments which have taken place during the years and which have parameters as outcomes which can be fully analyzed.

Spalling is an effect that takes place in the concrete surface exposed to fire. Multiple characteristics influence the appearance of spalling in concrete. These can be gathered in three categories: material property, mechanical contour condition and thermal exposure. To numerate them it can be said that three phenomenon's where taking place: thermos-hydraulic, thermos-mechanical and thermos-chemical. Although this phenomena sure influence the appearance of spalling it is not known how each of the relations between each other, as well as with themselves, induces spalling.

The phenomenon of thermo-hydraulic mechanism results from the transport or evaporation of capillarity water in the concrete micro structure. Higher moisture increases spalling. Also, micro PP fiber if believed to reduce the spalling effect because when it melts physical channels are created and water flows out of the mix through there.

On a micro scale, and related to thermo-hydraulic mechanisms, spall is associated with internal stresses by incompatibility of thermal expansion and mechanical properties such as aggregates and cement. On the macro scale, results from mechanical loads, contour conditions and uneven heat exposure presence of cold areas. Also, the specimens dimensions.

The phenomenon of thermo-chemical mechanisms has had little studying from researchers, but it is obvious that concrete properties when exposed to heat suffer degradation of the components.

It can be seen that we are dealing with a complex effect that is influenced by many parameters: moisture content, aggregates, curing, compressive stress and compressive strength, water to cement ratio, age of the specimen, heating technics, mechanical loads, density, permeability, silica fume, pore pressure, fibers.

1.4. Project Objectives

The objective of the projects are divided in two sections:
Experimentation:

- Expose samples to fire: plain concrete, concrete with plastic fibers, concrete with polypropylene, and with steal. Analyze how much surface spalled.
- Temperature analysis with thermocouples
- Cutting samples into 5 cores and do visual analysis of the concrete (color degradation)
- Cutting each of those 5 cores into 3 parts one of which the one closer to the fire had no purpose. The other two where tested in compression or tension and analysis of the results.

Theoretical analysis:

- Establish relationship between the parameters that influence spalling
- Develop a model that can simulate the spalling effect with an input of the material properties, the heat flux and the external conditions.

1.5. Methodology

The thesis follows a methodology divided in two:

Experimentation:

- Visual testing
- Data analysis
- Compression and tension testing

Theoretical:

- Articles to establish parameters and state of the art
- Ansys
- Matlab: to develop a model that can predict the spalling effect and the mechanical properties of the material after the hazard.

The resources used are:

- Previous researches
- Ansys
- Matlab

2

State of the Art

"The secret of success is constancy to purpose." Benjamin Disraeli

---

The main objective of this project is to understand the spalling phenomenon. Since this event is not yet fully understood it is of high importance to understand the experiment which have taken place during the years and which have parameters as outcomes which can be fully analyzed. The main objective of the chapter is to understand the relationship between all the parameters influencing spalling. For this, all the studies to date have been researched and analyzed.

2.1. Introduction

Concrete spalling is an effect produced in the external layer of the material when hight temperatures are reached. This effect is produced due to the water of the material evaporating and needing to scape, the moisture. The pushing of the moisture through the concrete towards the outerlayer originates the material to break and explode out of its surface, making this event dangerous.

2.2. Eurocode

The Eurocode (EC) is a legal document which takes into account the effect of fire in the properties of concrete. These properties have to be taken into account when dimensioning a new infrastructure as a safety measure. The properties differ depending on the aggregate type in the mix. The aggregate used in The University of Queensland laboratory was basalt, which is a type of siliceous aggregate. All further data is considered with siliceous aggregate.

- Explosive spalling, the most dangerous type there is due to the concrete exploding put at high velocities, is unlikely to occur if moisture content is below k%. Begin k usually 3%. Above this constant the occurrence of spalling has to be studied.

- Density: as temperature increases the moisture content of the concrete decreases leading to a reduced density as temperature increases. At first it remains constant but as it reaches a value of 115ºC it falls linearly.

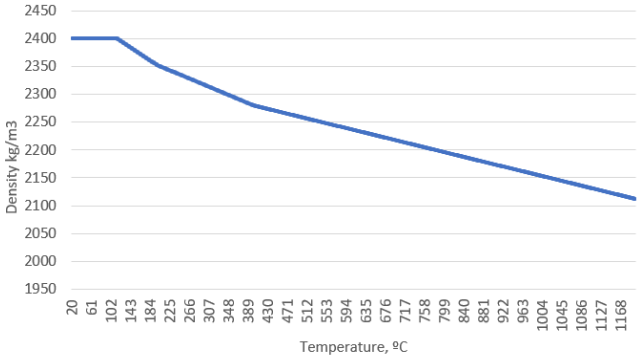

Figure 2.1. Relation between temperature and density by Eurocode.

- Specific heat: a really important property for the heat transfer problem to be solved. It has a peak which varies in relation to the moisture content of the concrete sample being u the moisture content.

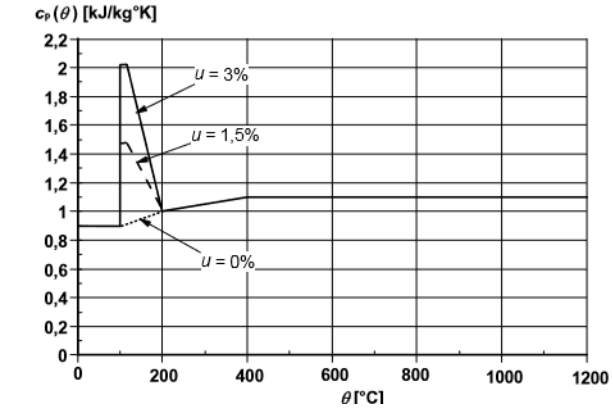

Figure 2.2. Specific heat of concrete by Eurocode.

- Conductivity: thermal conductivity is the ability of a material to transfer energy. For concrete it can be said that values vary between a lower and an upper limit.

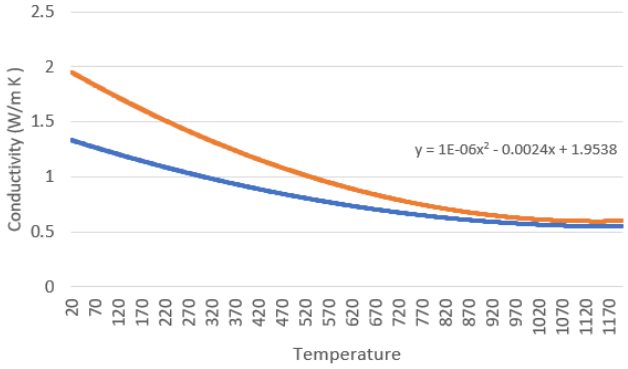

Figure 2.3. Conductivity of concrete by Eurocode.

- Thermal elongation: as mentioned before some parameters dependence on the type of aggregate in the concrete, Eurocode studies Siliceous an Calcareous aggregates. Our concrete a siliceous aggregate as the material used is Basalt.

- Modulus of Elasticity: the temperature value of the modulus is calculated from the compressive strength of out testing sample (28 days) which resulted 52.86MPa. By means of the formula

$$E = 4700 * \sqrt{52.86} MPa$$

the Elastic modulus at ambient temperature resulted 34171,3 MPa.

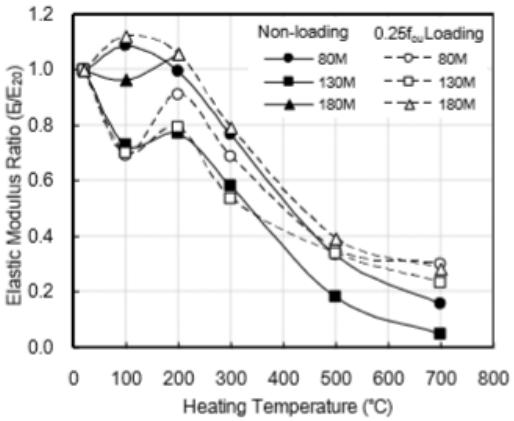

Figure 2.4. Elastic Modulus of concrete with increasing temperature.

- Compression: The ambient temperature of compressive strength was obtained from the test carried out in the laboratory.

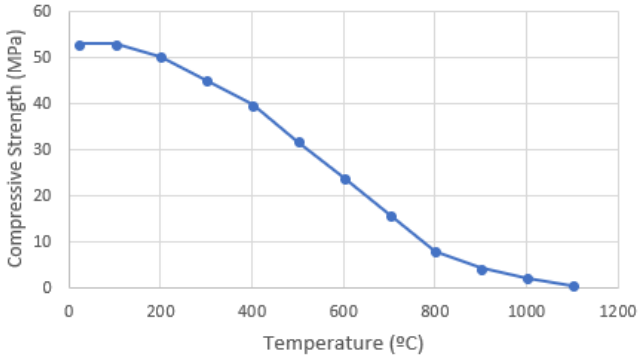

Figure 2.5. Variation of compressive strength of concrete by Eurocode.

- Tensile Strength

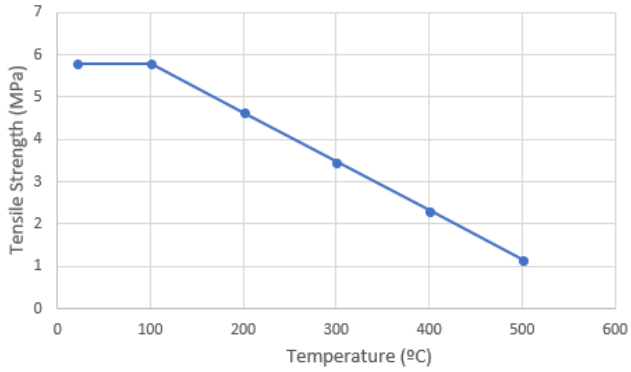

Figure 2.6. Variation of tensile strength of concrete by Eurocode.

- Thermal Expansion of concrete for siliceus aggregate

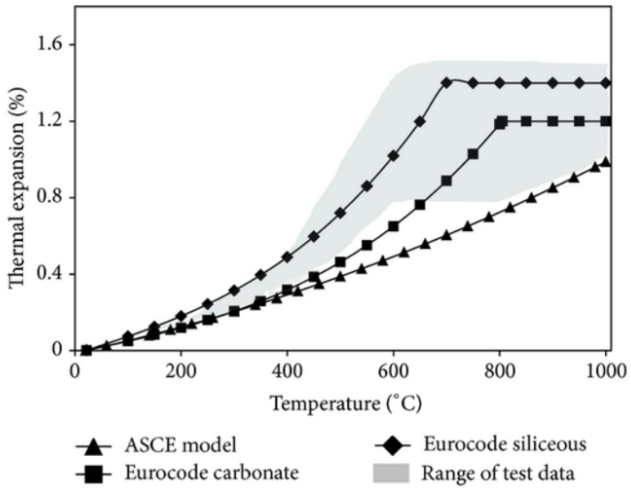

Figure 2.7. Thermal expansion of concrete by aggregate concrete by Eurocode.

There are multiple parameters which affect spalling, the Eurocode enumerates the following external parameters such as fire temperature curve, heat exposure, external load; dimensions and reinforcement of the sample (geometry, concrete cover thickness, reinforcement); concrete composition such as aggregate, cement, filter, air content, fibre content, moisture content (very difficult to measure), permeability, strength properties, silica fume (for concrete strength less than 80MPa, silica fume less than 6% by weight of cement spalling is unlikely to occur).

2.3. Previous Concrete Spalling Studies

This section analyses the concrete spalling experimental studies produced since the early 1900s.

Miller 1906: failure rate and great amount of spalling were because of the high moisture content of the concrete associated to the early age at the time of testing. "Uncombined water which was converted into steam and caused the disruption of the concrete". Solution proposed: "necessary to guard against the occupancy of concrete structures within the time required for the concrete to appropriate all its water".

Hull and Ingberg 1925: spalling related to the thermos-mechanical behavior of certain mineral constituents known as "spalling aggregates"

Meyer-Ottens 1965: spalling was characterized for its aggregate spalling, surface spalling, destructive spalling. The most significance occurrence of spalling was the thickness of the slab.

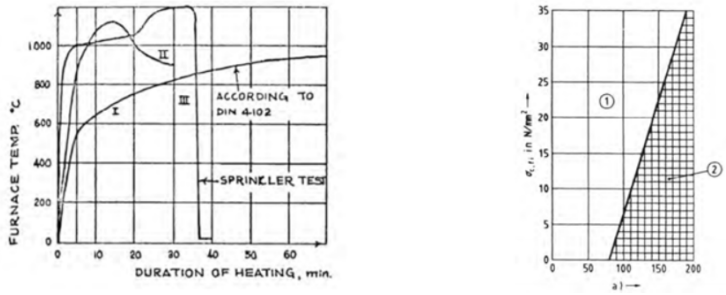

Figure 2.8. Meller-Ottens 1965, Heat exposure and risk of spalling.

Akhtaruzzaman and sullivan 1970: water cured specimens show an increase susceptibility to spalling over moist-cured specimens (all specimens were studied at 28 days or less). Spalling occurred when the measured temperature was 165-200ºC.

Dougill 1971: lack of spalling related to the small aggregate size used. Although this study states that early age concrete is less likely to show spalling it has now been shown that early age concretes are associated to higher moisture thus more spalling.

Christiaanse et al. 1972: high compressive stress plus high moisture increases the occurrence of spalling. Also, no spalling shown for concretes with moisture contents lower than 2% by mass.

Zhukoc 1975: Spalling more likely in concretes with high water-to-cement ratios, high moisture content, high strength, and low porosity.

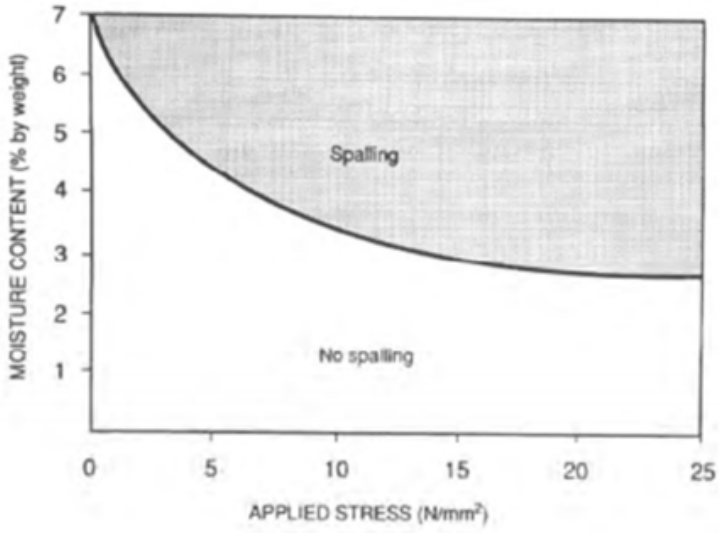

Figure 2.9. Zhukoc 1975, Spalling relation with moisture content.

Sertmehmetoglu 1977: maximum pore pressures directly proportional to the depth and age of the test specimen (thicker and older specimens display higher maximum pore pressures). Spalling always occurred for specimens kept under water for the seven first days after casting. Cracks parallel to the heater surface appeared for specimens under biaxial compression.

Chandra et al. 1980: composition concrete mix influences risk of spalling. Addition of 1.5% of polymer (by weight of cement) was sufficient to avoid spalling.

Copier 1983: Moisture content (most important factor in spalling), aggregate type, applied compressive stress, compressive strength, reinforcement ratio, and heating condition investigates (others influence but less). Moisture content below 7% by volume (or 3% by mass) which is reached by concrete in centrally heated buildings after 2-5 years: suggesting not to occupy concrete structures until the appropriate moisture level was achieved. Smith 1991: cellulose based fueled fires induce spalling; gasoline fires do not.

Sanjayan and Stocks 1993: high strength concrete more prone to spalling than normal strength concrete. Spalling occurs in initial stages of a fire. Less spalling occurs in areas with wider flexural cracks and structural shapes heated on multiple faces.

Connolly 1995: Spalling is promoted in:

- higher incident heat flux and higher applied mechanical loads
- axial loading rather than biaxial
- higher water-to-cement ratios
- Lower compressive strength
- Reduction in specimen thickness
- Pre-dried specimens with 0% moisture can spall under certain conditions (moisture alone cannot demonstrate spalling)
- High number of fines or added micro-silica
- Observed probability of explosive spalling is quite erratic. Not only explained by inherent chaotic influences but also due to an inconsistency in the number of specimens tested under various conditions?.

Shuttlewoth 1997: spalling is more likely:

- Lightweight aggregate
- Including mono filament PP fibers reduces spalling
- Steel fibres -> no obvious effect
- 2001: mono filament polypropylene fibers significantly reduce the risk of explosive spalling when exposed to severe hydrocarbon fires.

Chan et al. 1999: Main factors are moisture content and strength. When strength is higher than 60 MPa the higher the moisture content the greater the spalling probability

Morita et al. 2000: Spalling was more likely:

- Lower water-to-cement ratio
- One year old specimen more likely than 2 months old
- Spalling does not or only slightly occur in unreinforced concrete columns
- Preventing spalling with polypropylene fibres

- More spalling in a slow heating time-temperature curve than with the standard time-temperature curve (CEN 2012)

Ali et al.2004: conclusions:

- Spalling occurs within the first 45 min of the test
- Applied load has no influence on spalling
- In unrestrained columns the strength of concrete has no influence
- Normal strength concrete show a higher degree of spalling than unrestrained
- Low heating raters-> lower spalling (contradicting Morita 2000)
- Critical factor is the random distribution of voids inside the concrete mass.

Bilodeau 2004: studying the minimum content of PP fibers for which no heat-induced concrete spalling could be assured and optimizing the amount of PP fiber needed. Susceptibility of the concrete spalling increases with the degree of absorption of the lightweight aggregate included in the mix. 3,5kg per m^3 of the 20mm fiber were needed and only 1.5kg per m^3 of the 12,5mm fiber. Concluding that this was due to the thinner appearance of the fiber.

Hertz and Sorensen 2005: thinner PP fibers are more effective in lowering the spalling risk. Differential thermal stresses between aggregates and cement are unlikely to be a main factor which influences the occurrence of heat induced spalling.

Phan 2007: PP fibres reduce the probability of spalling causing a reduction in the measured maximun capillarity pore pressure. Lower capillarity pore pressure occurred for specimens under higher heating rates. Higher thermal gradients (by high heating rates) might cause micro crack to develop early allowing pore pressure to escape and resulting lower maximun pore pressure?. Critical capillarity pore pressure [2.02,21]MPa. Higher water-to-cement ratios and lover moisture spall less.

Larbu 2008: after PP fibres were evaporated these left physical channels believe to improve the moisture transport and there for prevent spalling.

Zeiml 2008: three types of spalling:

- Explosive: v>14m/s
- Progressive spalling: reduced velocities. Fall-off of concrete pieces with gravity as the acceleration

  Conclusions:

- Volume and velocity of the spalled-off pieces are inversely proportional
- Thicker spalled-off pieces were driven by the thermos-mechanical process while smaller with higher velocities (driven by thermos-hydro process)
- Predict spalling: thermos-hydro and thermos-mechanical must be considered

Jansson and Bostrom 2010: ?pressure in the capillarity system is not the driving force for spalling during fire exposure of the investigated concretes, there for it contradicts with the addition of PP fibers reduces spalling because of the reduction of capillarity pore pressure due to the creation of physical channels which allow moisture to scape.

Ko 2011: lower water-to-cement ratio and curing humid conditions promote spalling.

Mindeguia 2010::concrete cracking limits the built-up of pressure. Capillarity pore pressures is not the only driver.

RILEM Spalling workshop:

Reference[1]	Type of Specimen and Dimensions	Thermal Exposure Apparatus	Thermal Conditioning	Mechanical Conditioning
Jansson and Boström 2011	Large scale prestressed and reinforced beams	Standard fire resistance furnace	Cellulosic curve (CEN 2012) and 10°C/min	Loaded and unloaded
Tanibe et al. 2011	Cylinders (300 mm Φ, 100 mm high)	Not specified	RABT ZTV tunnel (car) curve (NFPA 2014)	Restrained
Husinann et al. 2011	Non-reinforced slabs (600×600×300 mm^3)	Standard fire resistance furnace	Hydrocarbon curve (CEN 1999)	Unloaded
Albrektsson et al. 2011	Non-reinforced slabs (600×500×200 mm^3)	Small gas-fired furnace	Cellulosic curve (CEN 2012) and 10°C/min (< 1300°C)	Loaded
Klingsch and Frangi 2011	Cylinders (150 mm Φ, 300 mm high)	Electric furnace	1.5, 3 and 8 °C/min (< 700°C)	Unloaded
van der Heijden et al. 2011	Cylinders (80 mm Φ, 100 mm high)	Halogen lamps	12 kW/m^2 incident heat flux	Unloaded
Bamonte et al. 2011	Small prisms (80×80×500 mm^3)	Electric furnace	Sudden exposure to the pre-heated furnace at 750°C (*"simulates the first 20min of an hydrocarbon curve"*)	Unloaded

Figure 2.10. Rilem workshop table 1.

Reference[1]	Type of Specimen and Dimensions	Thermal Exposure Apparatus	Thermal Conditioning	Mechanical Conditioning
Hager and Zdeb 2011	Small prisms (40×40×80 mm^3)	Electric furnace	0.5, 1.0, and 2.0 °C/min	Unloaded
Vermeer et al. 2011	Not applicable	Mobile gas-fired burners	Constant 1250°C with an steep initial ramp (750 °C/min)	Not applicable
Alonso et al. 2011	Small cubes (100 mm)	Not specified	Cellulosic curve (CEN 2012), and 2 and 8.5 °C/min (< 1050°C)	Unloaded
Kirnbauer and Schneider 2011	Small prisms (300×250×100 mm^3)	Direct flame impingement from a gas-fired torch	*"Simulates"* the first 30 min of the cellulosic and hydrocarbon curves (CEN 2012)	Unloaded
Ehlig and Hothan 2011	Large scale reinforced slabs	Standard fire resistance furnace	Cellulosic curve (CEN 2012)	Loaded
Boström and Jansson 2011	Non-reinforced large scale slabs and small-scaled slabs (600×200×200 mm^3)	Standard fire resistance furnace and small gas-fired furnace	Cellulosic (CEN 2012) and hydrocarbon curve (CEN 1999)	Loaded
Pereira et al. 2011	Reinforced and non-reinforced slabs (600×600×300 mm^3)	Standard fire resistance furnace	Cellulosic (CEN 2012) and hydrocarbon curve (CEN 1999)	Unloaded

Figure 2.11. Rilem workshop table 2.

Reference[1]	Type of Specimen and Dimensions	Thermal Exposure Apparatus	Thermal Conditioning	Mechanical Conditioning
Ye et al. 2011	Non-reinforced slabs (300×300×150 mm^3)	Standard fire resistance furnace	Cellulosic curve (CEN 2012)	Unloaded
Grosse et al. 2011	Non-reinforced slabs (700×700×350 mm^3)	Standard fire resistance furnace	Cellulosic curve (CEN 2012)	Unloaded
Debicki et al. 2011	Spheres (120, 180 or 240 mm in diameter)	Electric furnace	5 °C/min (< 600°C)	Unloaded
Arai and Furuichi 2011	Large scale and medium scale reinforced slabs	Standard fire resistance furnace	RABT ZTV tunnel (train) curve (NFPA 2014)	Loaded and unloaded
Song et al. 2011	Cylinders (110 mm Φ, 200 mm high) and prisms (300×300×100mm^3)	Direct flame impingement from an LPG-fired torch	Flame temperature estimated to be at 1300°C	Unloaded
Saravanja et al. 2011	Cylinders (50 mm Φ, 100 mm high)	Not specified	2 and 5 °C/min (< 800°C)	Loaded
Knack 2011	Small cubes (100 mm)	Annealing oven	Sudden exposure to the pre-heated furnace at 1100°C	Unloaded

Figure 2.12. Rilem workshop table 3.

2.4. Theoretical Studies

This section, as well as the previous one analyses new studies but theoretical ones.

Harmathy 1965: spalling occurred by the pressure of the saturated layer. The transient penetration of heat into concrete results in desorption (changing from a adsorbed state on a surface to a gaseous or liquid state) of moisture in a layer adjoining the surface exposed to heat which was reabsorbed in colder regions downstream from the heat wave. As the heat reaches further in the concrete a saturated layer forms and transiently moves towards colder regions due to pressure difference.

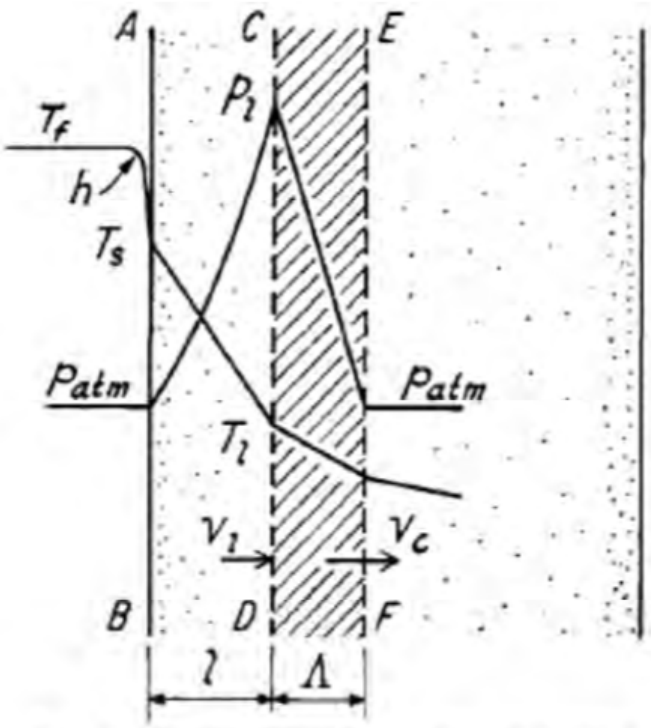

Figure 2.13. Moisture clog formation by Harmathy..

Meyer-Ottens 1972: against Harmathys´s theory Meyer-Ottens states that the moisture clog is formed at the boundary between dried and moist zones and evaporates as the heat wave moves forward. Spalling occurs when the tensile strength of the concrete is overcome by forces because of the moisture clog.

Saito 1965: the reason for explosive spalling in fire is that the thermal stress of the member grown higher than the compressive strength of concrete and results in the compressive failure. Spalling is caused due to differential thermal stresses close to the exposed surface.

Dougill 1971: spalling due to thermal expansion effects, causing cracking in planes parallel to the heated surface and promoted by high capillarity pore pressure in the concrete. Two failure modes: material outside the crack becomes unstable; and, cracks are filled with vapour which with enough pressure results in fracture.

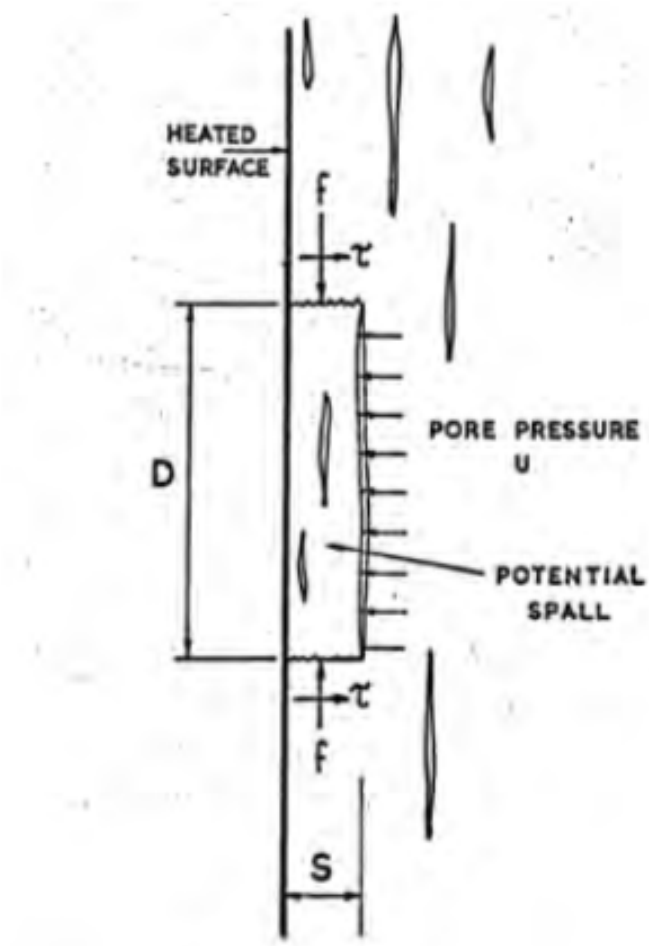

Figure 2.14. Dougill 1971, explanation of stress action on spall.

Zhukov 1975: pore pressure, thermal stresses and external mechanical conditioning were studied, and results showed that spalling occurred when a critical pore pressure was reached.

Bazant 1997: cracks parallel to the surface start forming increasing enormously the volume of vapor water available. Water is forced to expand but cannot reach the crack from the element concrete, capillarity pore pressure drops to zero and cracks start to open. Capillarity pore pressure does not lead to spalling, it only helps to trigger a crack. When a crack opens the concrete becomes unstable and leads to spalling. High strength concretes are more likely to spall than normal ones.

Khoury and Anderberg 2000: spalling occurs combining pore pressure, compression in the exposed surface and internal cracking.

Smith and Atkinson 2010: looking back most research was predominant in hydro influence but there is an effect of aggregate expansion caused by thermal incompatibility stresses.

2.5. Describing Spalling

As reviewed before both in theoretical and experimental studies, there are multiple characteristics that influence the appearance of spalling in concrete. These can be gathered in three categories: Material property, mechanical contour condition and thermal exposure. The following table made by Christian Maluk in this thesis groups these factors:

Category	Factors having an influence on increased heat-induced concrete spalling
Material Property	Lower age Increased moisture content Higher compressive strength Lower tensile strength Certain types and sizes of aggregates (e.g. siliceous aggregates) Certain types of cement (e.g. fine particle cement) Lower water-to-cement ratio Certain admixtures inclusion (e.g. fly ash, silica fume) Absence of polypropylene or steel fibres Certain casting techniques (e.g. vibrated concrete, SCC, spun concrete) Lower air-entrainment
Mechanical Conditioning	Certain internal reinforcement (e.g. type, ratio, tie configuration) Certain structural forms (e.g. shapes, sizes, thicknesses, spans) Higher in-service mechanical stress conditions
Thermal Exposure	Higher heating rates Certain heating techniques (e.g. gas-fired or electric-powered furnace, etc.) Single versus multi-surface exposures

Figure 2.15. Categorization of factor which affect spalling.

The results of these experimentations showed that three phenomenons where taking place: thermos-hydraulic, thermos-mechanical and thermos-chemical. Although these phenomena sure influence the appearance of spalling it is not known how each the relations between each, as well as with themselves, induces spalling.

2.5.1. Thermo-hydrauluc mechanisms

This phenomenon results from the transport or evaporation of capillarity water in the concrete microstructure. Higher moisture increases spalling. Also, micro PP fiber if believed to reduce the spalling effect because when it melts physical channels are created and water flows out of the mix through there

2.5.2. Thermo-mechanical mechanisms

On a micro scale, spall is associated with internal stresses by incompatibility of thermal expansion and mechanical properties such as aggregates and cement. On the macro scale, results from mechanical loads, contour conditions and uneven heat exposure presence of cold areas. Also, the specimens dimensions.

2.5.3. Thermo-chemical mechanisms

This phenomenon has had little studying from researchers, but it is obvious that concrete properties when exposed to heat suffer degradation of the components.

2.6. Quantification of the appearance of spalling

Arup Fire 2005 have quantified the risk factors for spalling shown in the following tables:

Key variables likely to promote spalling	Condition of the variable	Risk Factor
Compressive strength	> 55 MPa	Not quantified
	< 55 MPa	1
Heating rate	Hydrocarbon fire	5
	Cellulosic fire	1
Moisture content	> 3%	5
	< 3%	1
Presence of reinforcement	None	3
	Included	1
Cover to the reinforcement	> 40 mm	3
	< 40 mm	1
Aggregate type	Siliceous	3
	Calcareous	1
No. of Sides exposed	> 1	3
	= 1	1
Section size	< 200 mm	3
	> 200 mm	1
Mechanical restraint	Restrained	3
	Unrestrained	1
Thermal expansion	$> 10 \times 10^{-6}$	3
	$< 10 \times 10^{-6}$	1
External mechanical load	Loaded in compression	3
	Unloaded	1

Figure 2.16. Variables which affect spalling quantified by Arup Fire 2005.

Category	Risk of spalling	Value of Total Risk	Key Factors	Spalling Level
A	Very low	< 11	Ordinary strength, NWC, Unloaded, Unrestrained, Standard fire exposure, Reinforced, moisture <3%, one side exposure.	Zero or minimal
B	Low	12 – 20	Ordinary strength, NWC, restrained, Standard fire exposure Significant number of key variables* likely to promote spalling.	Up to the level of the reinforcement
C	Medium	21 – 28	Ordinary strength, NWC, restrained, Standard hydrocarbon fire exposure :Small number of key variables* likely to promote spalling	3 mm/min
D	High	29 – 37	Ordinary strength, NWC, restrained, Standard hydrocarbon fire exposure Significant number of key variables* likely to promote spalling	7 mm/min
E	Very High	> 37	High design strength (>55 MPa), standard hydrocarbon fire exposure.	Unquantifiable

Figure 2.17. Arup Fire 2005, Spalling categories..

2.7. Parameters influencing spalling

Many concrete studies have been studied so as to gain a deeper understanding on the parameters that make concrete more or less prone to spall. The relocation of data dates from 1906 to 2017.

The measuring technical vary from: temperature measurement gauges, water-cooled heat flux gauges, capillary pore pressure gauges of types and sizes, high speed cameras, acoustic emission (AE), nuclear magnetic resonance, digital image correlation, stereo microscopy polarizing, liquid and gas permeability measurement, thermal imaging, transition mass loss.

The following figure shows how the parameters which are going to be explained in the chapter are related to one another and how the affect the higher probability of spalling.

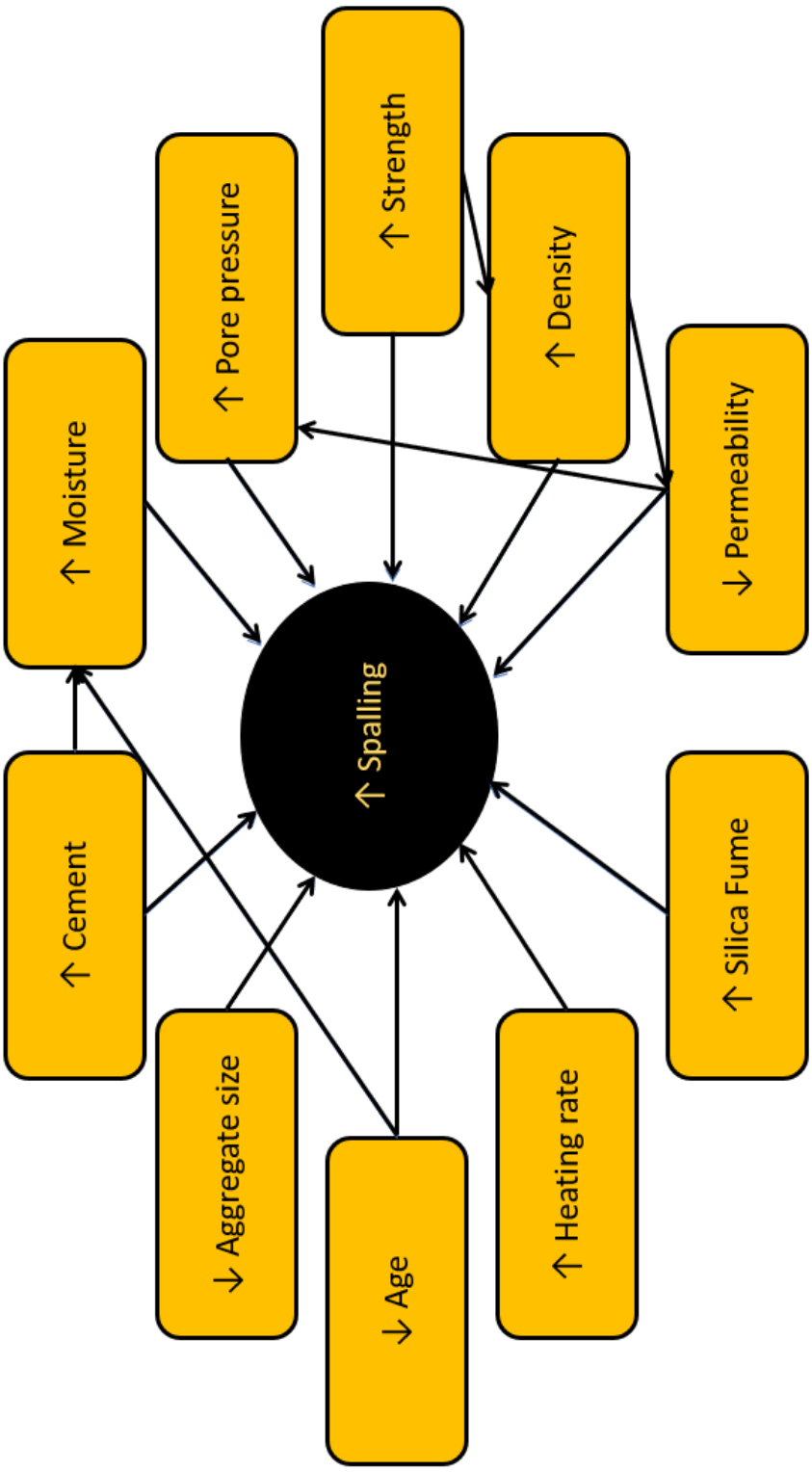

Figure 2.18. Relationship between spalling parameters.

2.7.1. Moisture content

Moisture content is one of the most important parameters when studying this phenomenon. Miller in 1906 stated that high moisture was associated to early age of the specimen and more spalling. Decades later numbers were established by researchers and most importantly by the Eurocode 2, Design of concrete structures. They established that when the moisture content is lower than 3% by mass spalling is unlikely to occur. In spite of this, Connolly (1995) experiments with 0% moisture content and spalling does occur demonstrating that this parameter cannot be studied alone. It influences thermal properties: density, thermal conductivity.

In spite of this, it has been demonstrated that some parameters depend on moisture content: shape (small sample quicker moisture decrease), size, rate and duration of heating (more cracks were moisture escapes with higher rates). At 105ºC concrete losses all its water but the chemical bound. At this temperature vapor pressure starts to increase (water boiling point) until the thermal micro cracks release all the pressure.

2.7.2. Aggregates

When considering aggregate two variables should be taken into account: type of aggregate and the size.

Firstly, the EC presents data for both siliceous and calcareous aggregates, as they behave differently. Siliceous aggregate (whose expansion leads to slight contraction) loses higher compression strength than calcareous (whose expansion leads to cracks) until 800ºC. Also both Shuttlewoth (1997) and Bilodeau (2004) both concluded that lightweight aggregate is more likely to present spalling.

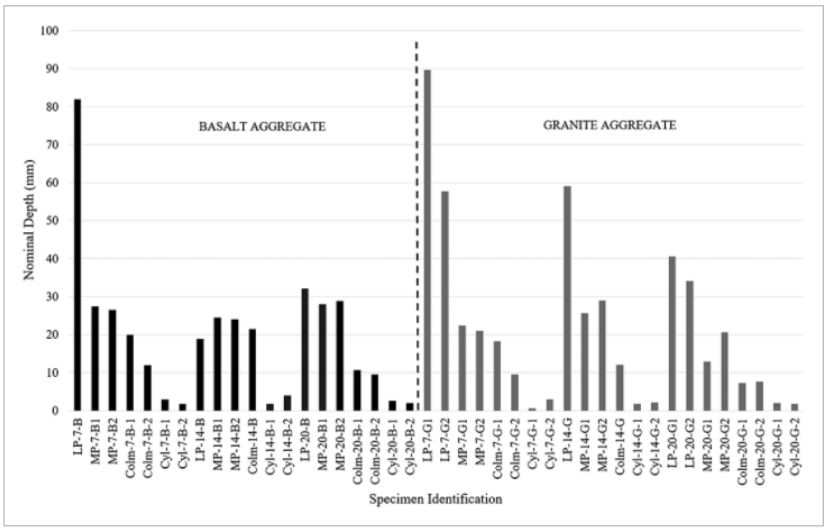

Figure 2.19. Depth of spalling with different concrete aggregates.

Secondly, the size of the aggregate generally influences as specimen size increases nominal spalling depth decreases, seen in 2.20

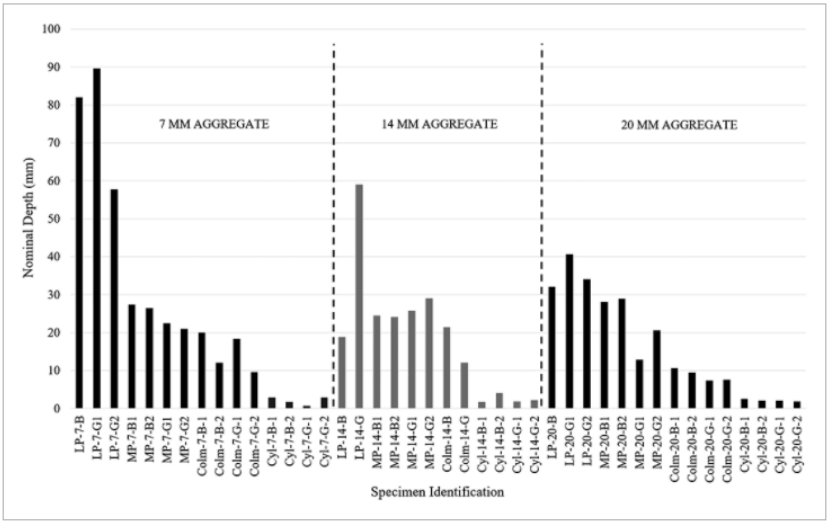

Figure 2.20. Depth of spalling when aggregate has different sizes.

2.7.3. Curing

Akhraruzzaman and Sullivan in 1970 stablished that water cured samples showed higher spalling than moisture cured.

Figure 2.21 shows the temperature at which specimens spalled related to the type of curing. It can be seen that autoclaved only spalles when the heating rate is significantly high and when it does spall the mean temperature is 271.7ºC.

Steam cured and water cured spall for a larger range of heating temperatures, having a lower spalling temperature (means 230,8ºC and 257,2ºC for 2ºc/min and 248,5ºC; 249,1ºC for 1ºC/min). Moreover, these researchers found that steam curing and autoclaving conditions presents ultra-high performance for cementitious material.

RPC curing conditions	heating rate				
	2.0 °C/min		1.0 °C/min		0.5 °C/min
		Spalling temperature		Spalling temperature	
cured in water (RPC_W)	all (4/4)	231 230 227 235	all (4/4)	238 257 283 220	none (2/0)
steam cured (RPC_S)	all (4/4)	253 262 253 261	all (4/4)	241 261 254 241	none (3/0)
autoclaved (RPC_A)	all (4/4)	267 299 273 250	none (4/0)		none (2/0)

Figure 2.21. Spalling when cured in different conditions by Izabela Hager and Tomas Zdeb.

2.7.4. Compressive Stress and compressive strength

Concrete exposed to high temperature decreases its compressive and flexural strength as temperature increases (when cooled in water the decrease is higher) with a simultaneous increase in the elastic modulus. Higher concrete strength leads to a higher probability of spalling because of a more compacted concrete member

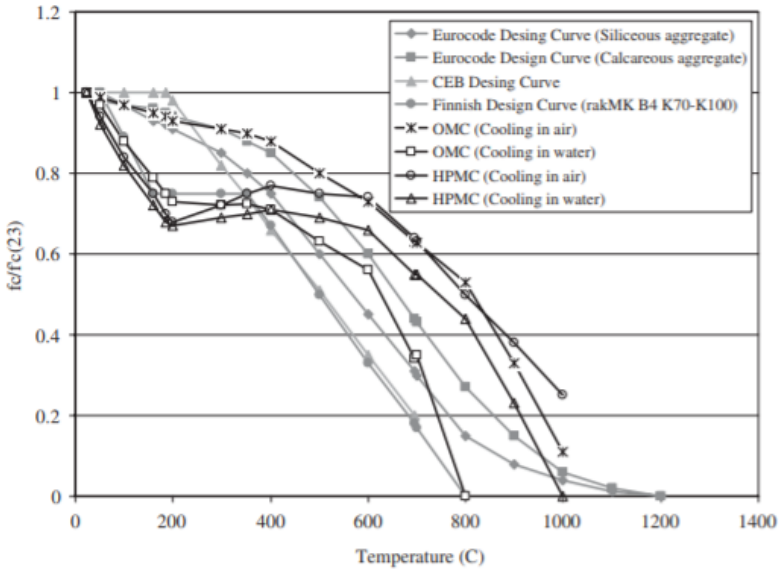

Figure 2.22. Variation of compressive strength with temperature by Metin Husem.

2.7.5. Water to Cement Ratio

The water to cement ratio is believed to be one of the main parameters influencing spalling.

Before serious researches were performed Zhukov (1975) and Connolly (1995) believed that high W/C concrete mixes promoted spalling. Yet, it has been studied that high W/C ratio reduces the spalling effect. There for the more amount of cement the more moisture available and higher the spalling.

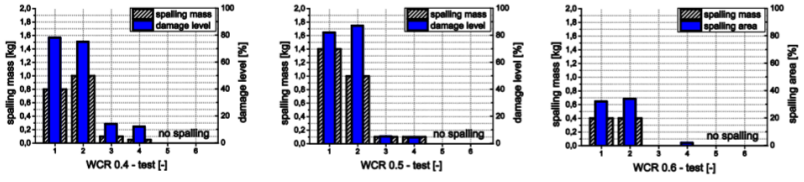

Figure 2.23. Spalling mass and damage level by Marcus Maier and Roman Lackner.

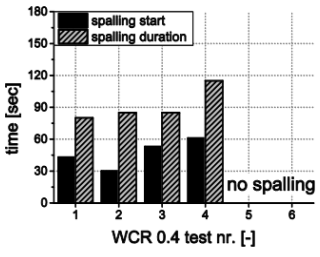

Figure 10: Spalling start and duration of WCR 0.4

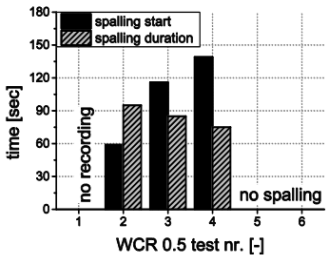

Figure 11: Spalling start and duration of WCR 0.5

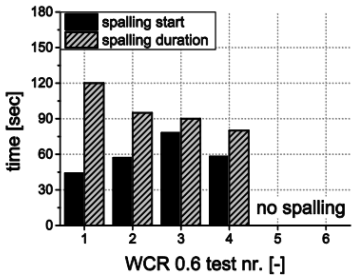

Figure 12: Spalling start and duration of WCR 0.6

Figure 2.24. Spalling start time and duration by Marcus Maier and Roman Lackner.

2.7.6. Age of Specimen

This is a parameter not taken into account by many researchers. Yet, this parameter influences greatly in concrete strength, percentage of hydration, amount of free moisture, permeability, porosity.

The water content in concrete is inversely proportional to the age. Younger specimens have a higher water content, when heated the mass loss is greater (more water to evaporate) hence, more susceptible to spall.

Spalling of high strength concrete appears not to be affected by age in a similar manner, due primarily, to its inherently low permeability.

2.7.7. Heating Techniques

- Standard fire resistance furnaces
- Gas/oil-fired furnaces
- Electric furnaces
- Annealing ovens
- Direct flame from a torch or gas-fired burners
- High power halogen lamps
- Electrical resistance heating coils
- Ceramic blankets, etc.

The academic community is divided in two opinions: one saying that higher heating rates result in greater risk of spalling and others state the contrary.

Heating rate has a major influence on the occurrence of explosive spalling. The probability, and severity of explosive spalling increase with increase of heating rate. Figure 2.25 confirms that higher heating rate provokes sooner spalling.

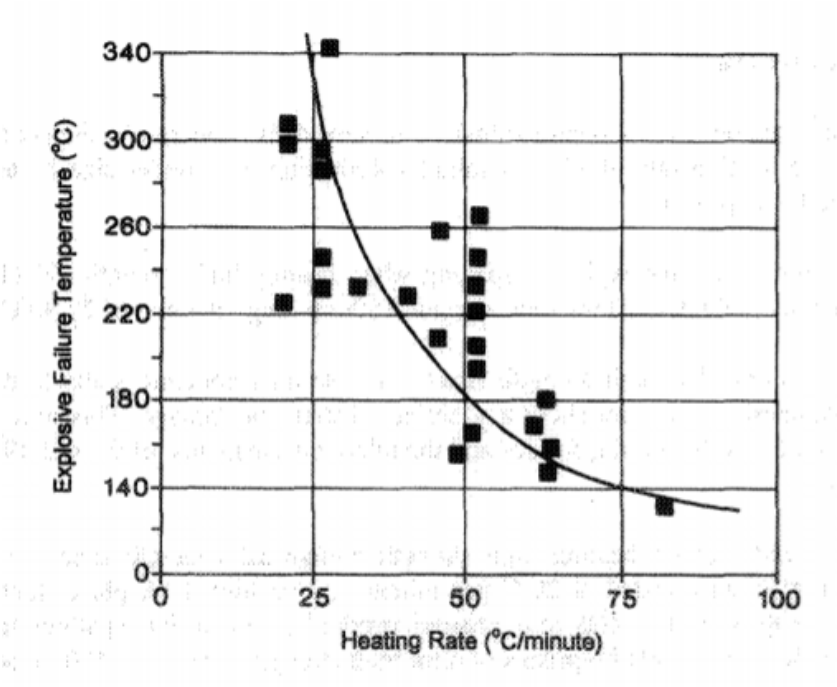

Figure 2.25. Temperature of the spall related to the heating rate.

When heat flux is applied in both sides is more likely to spall than when applied only in one side.

2.7.8. Mechanical Load

Most tests are performed without any load due to the large expense. Those which do apply a load are in a low scale. But despite all the research there are no validated conclusions.

It can be summarized that mechanical load should be limited. Increase in compressive stress has a negative impact.

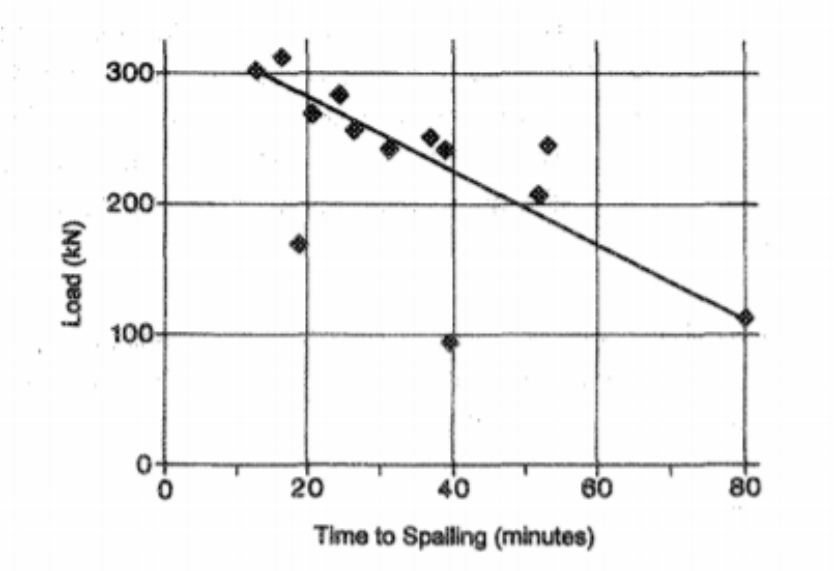

Figure 2.26. Effect of the load applied in the spalling time.

2.7.9. Density

Density divides concrete in two categories: lightweight aggregate (1350-1850[kg.m^3) and normal weight aggregate (2150-2450 kg.m^3). The differentiation on properties begins when the concrete reaches a temperature of 600^{o}C, up to that the material only experiences a 10% mass loss. Siliceous aggregate doesnt experience significant mass loss but carbonate aggregate does.

Marcus Maier and Roman Lackner (2017) state that denser concrete show higher damage. Kodur (2012) experienced that the strength of the concrete is not a influence factor; moreover, steel fibers affect spalling from 800ºC onwards reducing the mass loss compared to plain concrete.

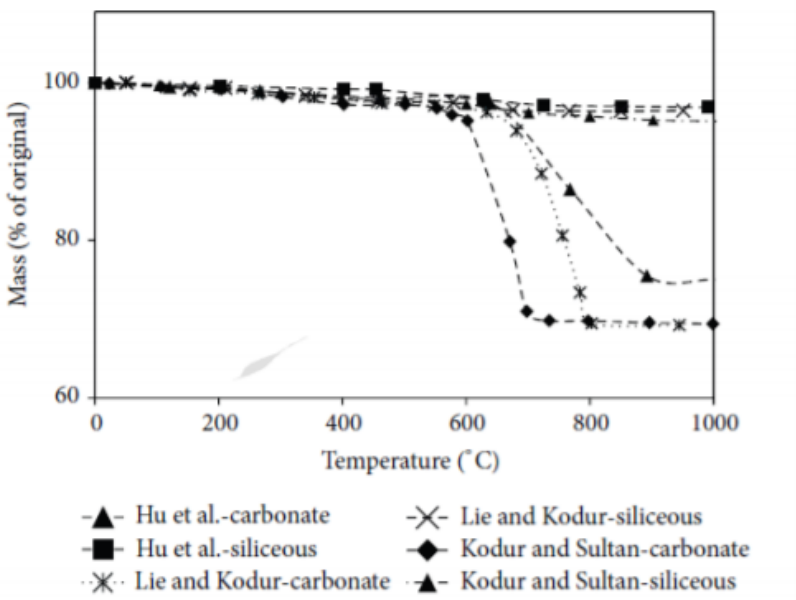

Figure 2.27. Variation of mass with rising temperature, Kodur 2012.

2.7.10. Permeability

Permeability is one of the main factors in concrete damage after fire. The lower the permeability the higher the damage caused by spalling.

After the heating process, the concrete that spalled showed that permeability increased disproportionately higher after heating them from 105-300ºC compared to concretes which did not spall. The presence of PP fibers makes permeability to increase faster, not only due to the melting fibers but to the crack formation.

Permeability increases due to crack formation, increase in porosity and interconection of pores because of microcracks, the lower the size of the aggregate the higher the permeability.

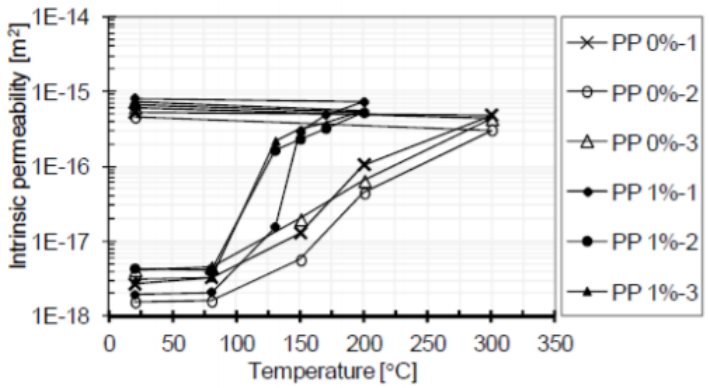

Figure 2.28. Temperature influence in permeability of concrete.

2.7.11. Silica fume

High strength concrete (HSC) is made with the addition of silica fume. This substance makes concrete denser. Denser concrete spalls easier because of the reduction of permeability which blocks the release of pore pressure with increasing temperatures.

2.7.12. Pore pressure

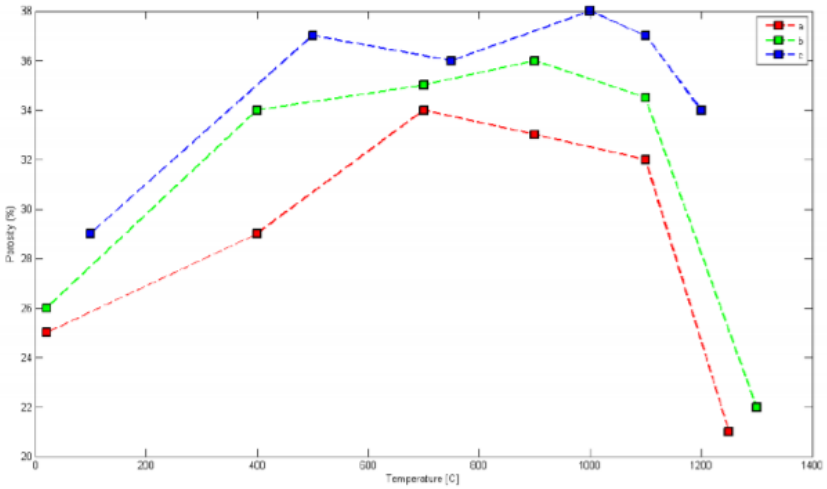

Figure 2.29. Temperature influence in concrete porosity, Bazant and Kaplan (1996).

In the figure by Bazant and Kaplan (1996) two events should be pointed out:

- Significant increase in porosity due to pore size expansion and apparition of micro cracks, starting at 500ºC to 900ºC.

- Significant decrease in porosity attributed to the decomposition of calcite, CO2 replaces hydraulic bonds.

The research by Singh (2016), where the relationship between pore pressure of concrete and elevated temperatures was studied, showed that the increase of pore pressure is related to the increase of concrete strength, because of the increase of density. As seen before, high density means more permeability and there for more pore pressure. Singh experimented with heating rates of 5, 10 and 25ºC/min and only 5, 25ºC/min showed spalling. When the rate is low pore pressure development governs the spall. When it is high, thermal stress is the cause of the spall and pore pressure does not take park in the phenomenon. The lack of spall on 10ºC/min heating rate is due to lack of sufficient pore pressure development and lack of thermal stress. Another factor influencing pore pressure is curing duration, as curing duration decreases pore pressure does too, because of low moisture content and initial cracks.

2.7.13. Fibers

For the past decades security measures have been established to achieve the reduction of spalling. The most common is the addition of polypropylene (PP) fibers in the concrete mixture. These fibers are believed to create channels, when they melt at around 170ºC, for moisture transport reducing the measured capillarity pore pressure.

The thinner the fibers the lower the spall.

Apart from PP other material are currently being studied such as steel, textile, recycled tire. Although steel fibers have no influence in spalling prevention (it might be because they do not melt) the mechanical properties in the residual concrete almost remain constant. These thesis studies the effect of steal, plastic and PP fibers the effect can be seen in chapter 3 .

2.7.14. Outcome

The traditional measurement after a fire test was performed on concrete including measuring the surface lost, depth reached, volume/mass spalled. Other less common measurements through thickness temperature, capillarity pore pressure, transient mass loss and acoustic emissions.

Type of spalling		Description
General or Destructive Spalling		Violent and occurs at an early stage of heating. This form of spalling causes extensive damage or complete destruction of a member. The occurrence of general spalling means a fire test is ended.
Local Spalling	Surface Spalling	Pitting, local blistering and local removal of material – sometimes violent.
	Aggregate Splitting	Failure of aggregate near the surface often accompanied by surface spalling.
	Corner Separation	Removal of external corners from beams and columns – occasionally violent.
Sloughing Off		This is a gradual progressive form of breakdown, involving partial separation of layers of surface material from the member that may continue slowly through the later stages of heating.

Figure 2.30. Types of spalling defines by Dougill, 1971.

Reference	Critical Temp. [°C]	Heating rate [°C/min]	Specimens type [mm]
Akhtaruzzaman and Sulivan 1970	165 – 200	9 – 11	Medium scale beam
Chandra et al. 1980	125 – 175	(ASTM 2012)	Medium scale slab
Castillo and Durrani 1990	320 – 360	7 – 8	Small cylinder
Hammer 1995	300	2	Small cylinder

Figure 2.31. Critical spalling temperatures defined before.

2.8. Types of Spalling

Spalling with all its characteristics can e studied depending on the location of the spall and the origin of the spall.

The location of the spall opens up to three categories:

- Aggregate Spalling: it is located in the surface hence no serious damage is caused, only superficially. Although when heated continuously it can harm the concrete permanently.
- Corner spalling: corners of member fall off when the specimen is heated from two or more adjacent size also due to thermal cracks. It is a dangerous form which occurs at late stages of spalling because it liberates all the reinforcement.
- Surface spalling: a very harmful type of spall, a large area burst out of the concrete member. It can extend through heat exposure occurring in the initial stages of fire.

The origin of the spall:

- Progressive spalling: heat is maintained for large stages exposing layer after layer when the previous is exposed because of the spalling.
- Explosive spalling: high pore pressure causes this spall (with popping sound and violent breaking), it is a dangerous type causing collapses of structural members losing large volume.

2.9. Conclusions

The state of the art is a basic and necessary procedure when it comes to understanding the phenomenons which we want to keep developing.

In this particular case, fire spalling has been studied for many years yet the outcomes have not been stipulated because there is a huge hole to be filled.

Many independent and dependent parameters influence the phenomenon. For this thesis it is of high importance to understand how the influence the apparition of spalling so as to implement each one on the numerical model for a reasonable outcome.

Concluding, thanks to the work of many researches of the past we can move forward with our study.

3

Experimentation

"Others may question your credentials, your papers, your degrees. Others may look for all kinds of ways to diminish your worth. But what is inside you no one can take from you or tarnish. This is your worth, who you really are, your degree that can go with you wherever you go, that you bring with you the moment you come into a room, that can't be manipulated or shaken. Without that sense of self, no amount of paper, no pedigree, and no credentials can make you legit. No matter what, you have to feel legit inside first."

3.1. Exposing concrete samples to high temperatures

The objective of the previous experimentation was to simulate the conditions of a fire to determine the behavior of the concretes with different fibers: discoloration of the samples, how much spalling, behavior of the fibers, and resistance of the concretes. There are six concrete mixes of which we tested two of each to have a more accurate approach of the data (12 blocks of concrete for testing):

- Mix 1: plain concrete
- Mix 2: incorporating BarChip fibers (7.0 kg/m^3)
- Mix 3: incorporating BarChip fibers (7.0 kg/m^3) and micro polypropylene fibers (1.0 kg/m^3)
- Mix 4: Plain concrete

- Mix 5: incorporating micro polypropylene fibers (1.0 kg/m^3)
- Mix 6: incorporating micro polypropylene fibers (1.0 kg/m^3) and steel fibers (35 kg/m^3)

These blocks were prepared in molds of 500x600x300 mm incorporating 13 temperature gauges which were incorporated to examine the behavior of each layer of concrete during not only the test time but also taking the data form the cooling stage. These thermocuples where placed as follows:

Thermocouples	Distance(mm)
TC1	1
TC2	5
TC3	10
TC4	15
TC5	20
TC6	25
TC7	50
TC8	75
TC9	100
TC10	150
TC11	200
TC12	250
TC13	300

Figure 3.1. Location of the thermocouples from the exposed surface.

3.2. Cores

To follow up the fire testing and due to the dimensions of the 12 original blocks being too grand for compression, tension and visual testing a technician cut each block into 5 cores (with the exception of mix 4 which only 3 cores were extracted). The positions chosen for the extraction were as close to the center as possible, since at the edges due to convention and conduction the results would not be accurate.

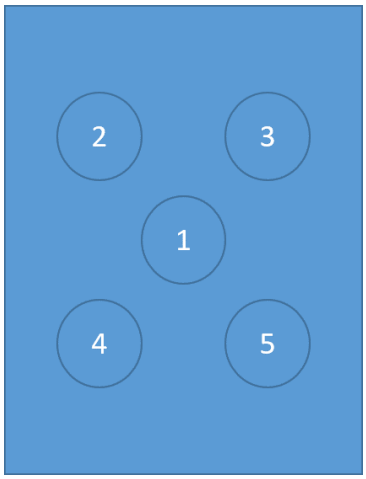

Figure 3.2. Position of the blocks extracted from each block.

The following pictures show the cores from all the samples:

Cores from sample 1A

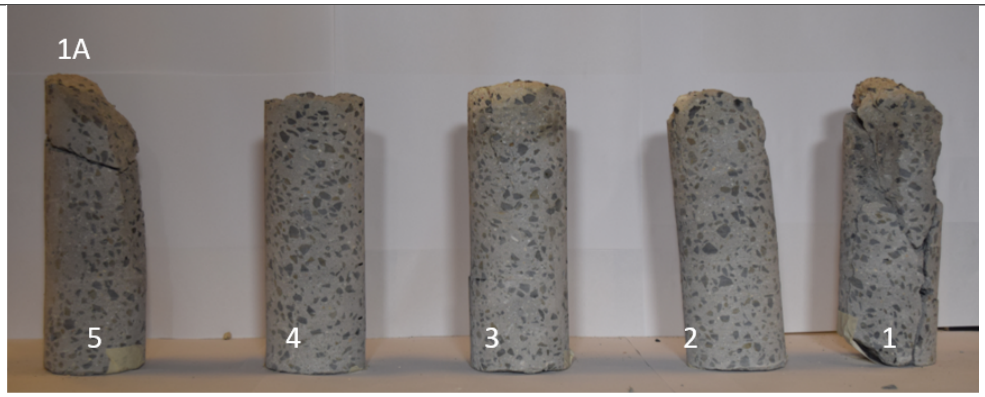

Cores from sample 1B

Cores from sample 2A

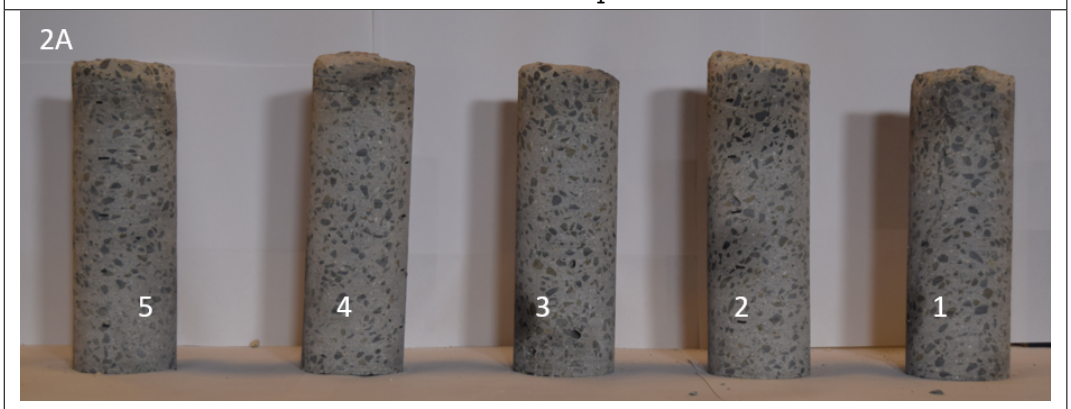

Cores from sample 2B

Cores from sample 3A

Cores from sample 3B

Cores from sample 4A

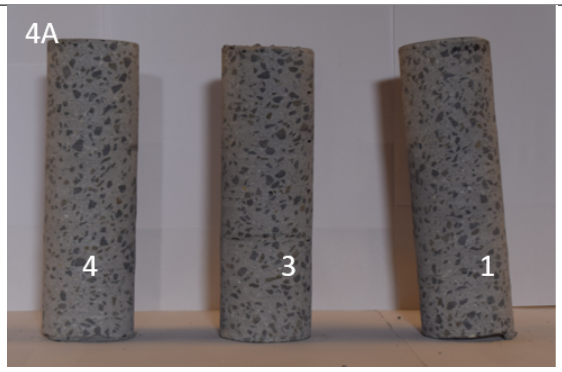

Cores from sample 4B

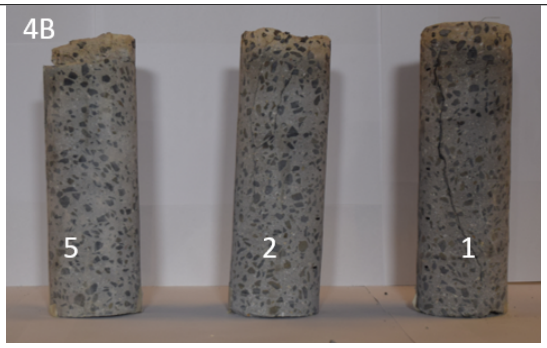

Cores from sample 5A

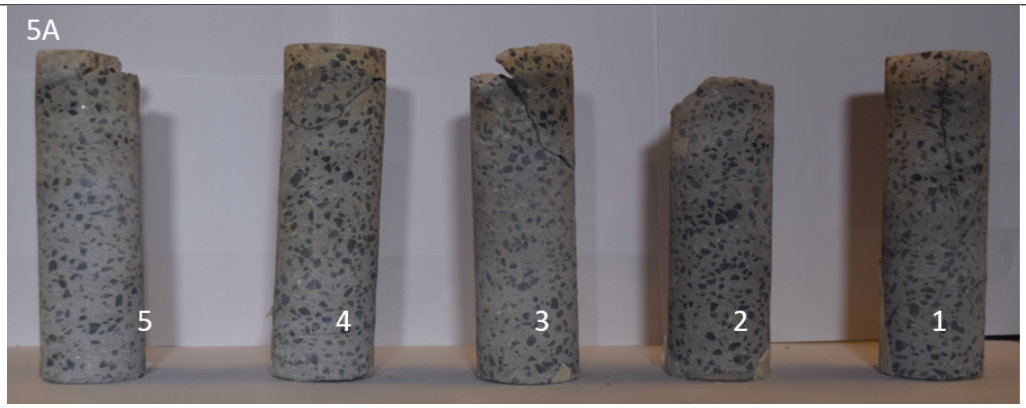

Cores from sample 5B

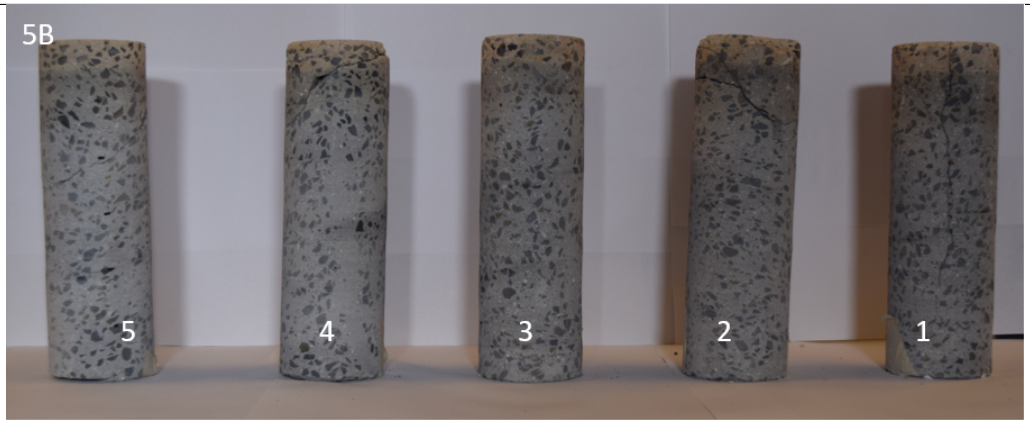

Cores from sample 6A

Cores from sample 6B

From these pictures, we can deduce that the fibers, both plastic and steel have a positive impact in preventing the detachment of the concrete. Spalling in concrete is when the material

has broken up, flaked or become pitted. This is caused by pressure created by a restriction on the movement of moisture steam.

Mix 1 and 4, non-fiber concretes, have a hard time staying in one piece. The lack of disrepair in the cores from the mix 4A is because this block was only summited to a minor time of intense heating.

Within the fiber mixes we can see that those containing micro polypropylene fibers are the ones with the best results in terms of spalling. These fibers help reduce the spalling of the concrete when at temperatures of 150°C the fibers begin to melt creating an amorphous polymer from the previous crystallinity. There are two theories on how these fibers help prevent the spalling.

On the one hand, Khoury believed that the steam overrides the expansion of the PP as it melts, to squeeze between the microfibre and the concrete matrix and pass along the length of the fiber. This is effective because of the total area occupied by the micro fibers and the conductivity of such fibers.

On the other hand, Sullivan claims that as fiber melts, its coefficient of thermal expansion is 8.5 times higher that the one of the concrete and these enables to create a large number of microcracks. If we gather all these microcracks together, form an interconnecting network that can facilitate the movement of steam through the concrete. This permeability, only created if a fire were to occur relieves the stresses created by the steam generation and counteracts the possibility of explosive spalling.

The part of the block exposed to the heat from mix number 2, only containing BarChip fibers, can be shown to be quite detached, this is because this fibers melt at temperatures of 130°. This is why a visual examination of where these fibers melted was carried out.

Visual test of the depth where the fibers where melted in 2A

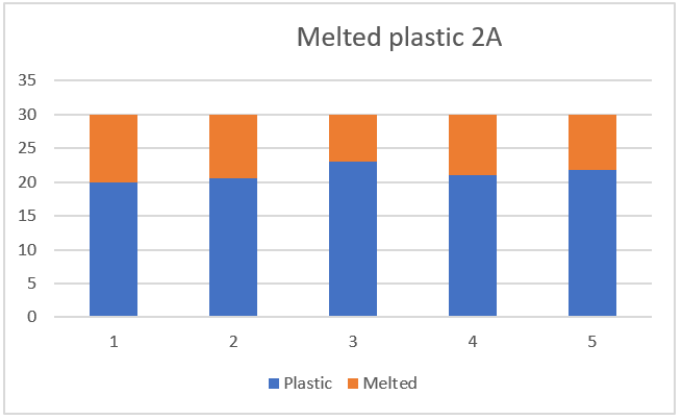

Visual test of the depth where the fibers where melted in 2B

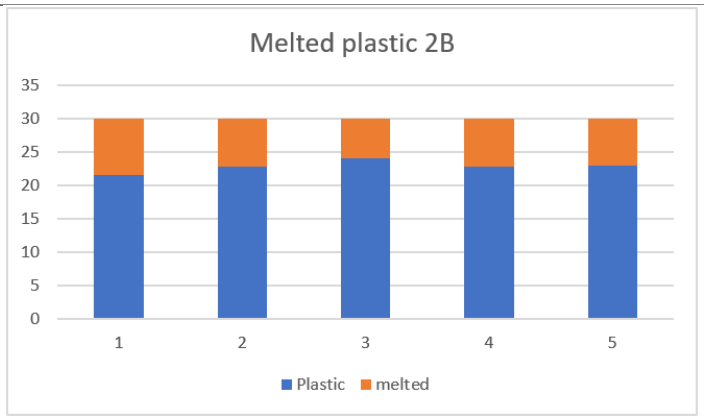

Visual test of the depth where the fibers where melted in 3A

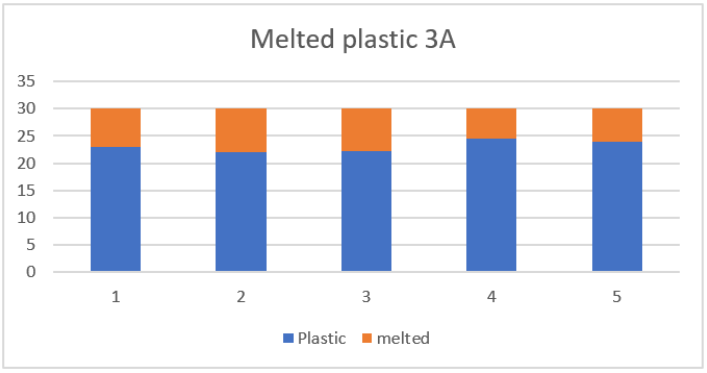

Visual test of the depth where the fibers where melted in 2B

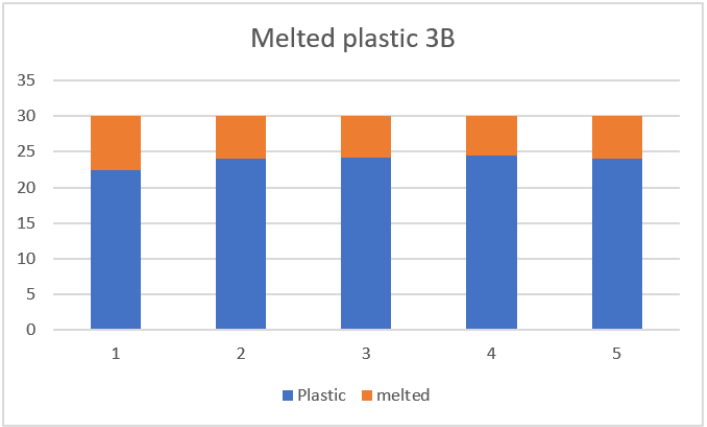

3.3. Decoloration

As we see from the figures in 3.2 after the explosion due to heat the part of the concrete that reaches high temperatures changes its color. Concrete is not affected by temperatures lower than 300°. Once this temperature is reached the resistance of the material decreases which is later not able to go back to its original resistance.

- 200 ^{0}C < T^a < 300 ^{0}C: loss of capillary water, no structural alterations nor decrease in the resistance.
- 300 ^{0}C < T^a < 400 ^{0}C: loss of the cement water. Superficial cracks show and a pink discoloration of the concrete due to the changes suffered by the steel compounds.
- 400 ^{0}C < T^a < 600 ^{0}C: loss of quicklime. Red color. Take into consideration that the mechanical properties of the concrete may decrease depending on the method used to extinguish the fire.
- 600 ^{0}C < T^a < 950 ^{0}C: detachment because of different dilatation coefficients. The concrete reaches grayish tones, losses inner water and becomes porous. These are the conditions where the loss of resistance may vary between 60%-90% which translates into a total substitution of the building.
- 950 ^{0}C < T^a < 1200 ^{0}C: destruction of the conglomerate getting a yellowish tone. No resistance what so ever.

Secondly, we can see that temperatures of 1400 ^{0}C were reached at the front part of the sample. This is why in the pictures it shows the yellowish tone mentioned above. Unfortunately, due to the spalling and high temperatures some thermocouples broke during the test. Some of these did not affect the final result because they broke during the cooling stage at a temperature lower than the maximum previously reached but some data was lost from other thermocouples which did break at an early stage of the experiment. In the following tables, which show the maximum temperature considering both the experiment and the cooling phase, we can see in a yellow color those thermocouples, which cannot be trusted.

Thermocouples	distance(mm)	Temperature max
TC1	1	1246.635
TC2	5	746.487
TC3	10	1371.917
TC4	15	1371.116
TC5	20	1371.792
TC6	25	1371.95
TC7	50	623.963
TC8	75	360.488
TC9	100	238.42
TC10	150	148.829
TC11	200	108.474
TC12	250	90.143
TC13	300	74.647

	time broke	Tembroke	relevant
broke	120.7839833	538.874	no
broke	4.22	89.264	no

Figure 3.3. Maximum temperature of each thermocouple in mix 1A..

Thermocouples	distance(mm)	Temperature max
TC1	1	427.506
TC2	5	394.682
TC3	10	
TC4	15	319.375
TC5	20	
TC6	25	
TC7	50	
TC8	75	
TC9	100	
TC10	150	
TC11	200	
TC12	250	
TC13	300	71.665

	time broke	tempbroke	relevant
broke	3.683466667	427.506	yes
Broke	4.683583333	394.682	yes
broke	6.418916667	319.375	yes

Figure 3.4. Maximum temperature of each thermocouple in mix 1B..

Thermocouples	distance(mm)	Temperature max	time broke	tembroke	relevant
TC1	1	470.944	3.870683333	461.801	no
TC2	5	934.33	5.624716667	854.037	no
TC3	10	0			
TC4	15	865.542	8.1082	865.542	yes
TC5	20	860.195	6.906166667	818.164	yes
TC6	25	452	5.855266667	452	yes
TC7	50	1006.159			
TC8	75	590.569			
TC9	100				
TC10	150				
TC11	200				
TC12	250	75.14			
TC13	300	59.724			
ext		31.146			

Figure 3.5. MMaximumax temperature of each thermocouple in mix 2A..

Thermocouples	distance(mm)	Temperature max		time broke	tembroke	relevant
TC1	1	378.922	broke	4.486	378.922	yes
TC2	5	176.883	broke	1.568083333	176.883	yes
TC3	10	555.43	broke	5.54	553.183	yes
TC4	15	422.006	broke	5.54	404.323	yes
TC5	20	171.706	broke	5.23625	171.211	yes
TC6	25	913.202				
TC7	50	650.362				
TC8	75	381.367				
TC9	100	203.67				
TC10	150	101.647				
TC11	200	68.951				
TC12	250	37.578				
TC13	300	29.116				

Figure 3.6. Maximum temperature of each thermocouple in mix 2B..

Thermocouples	distance(mm)	Temperature max		timebroke	tembroke	relevant
TC1	1	1344.787				
TC2	5	463.04	broke	4.05	463.04	yes
TC3	10	1028.543				
TC4	15	1371.704				
TC5	20	1370.899				
TC6	25	1293.135				
TC7	50	598.067				
TC8	75	347.455				
TC9	100	228.952				
TC10	150	123.885				
TC11	200	101.571				
TC12	250	79.269				
TC13	300	66.841				

Figure 3.7. Maximum temperature of each thermocouple in mix 3A..

Thermocouples	distance(mm)	Temperature max		timebroke	tembroke	relevant
TC1	1	414.16	Broke	4.4092	414.16	yes
TC2	5	320.604	Broke	4.4092	316.184	yes
TC3	10	1349.574				
TC4	15	376.012	Broke	6.21745	376.012	yes
TC5	20	1371.34				
TC6	25	1369.29				
TC7	50	469.215				
TC8	75	336.809				
TC9	100	246.158				
TC10	150	119.851				
TC11	200	87.179				
TC12	250	69.276				
TC13	300	59.218				

Figure 3.8. Maximum temperature of each thermocouple in mix 3B..

Thermocouples	distance(mm)	Temperature max
TC1	1	419.799
TC2	5	325.357
TC3	10	235.986
TC4	15	209.339
TC5	20	142.17
TC6	25	80.868
TC7	50	25.375
TC8	75	26.95
TC9	100	19.871
TC10	150	27.313
TC11	200	28.268
TC12	250	27.198
TC13	300	22.573

Figure 3.9. Maximum temperature of each thermocouple in mix 4A..

Thermocouples	distance(mm)	Temperature max
TC1	1	0
TC2	5	0
TC3	10	0
TC4	15	927.17
TC5	20	1168.312
TC6	25	678.886
TC7	50	494.722
TC8	75	258.212
TC9	100	0
TC10	150	109.788
TC11	200	87.068
TC12	250	65.619
TC13	300	56.517

Figure 3.10. Maximum temperature of each thermocouple in mix 4B..

Thermocouples	distance(mm)	Temperature max
TC1	1	931.664
TC2	5	904.899
TC3	10	1150.502
TC4	15	811.91
TC5	20	761.937
TC6	25	731.092
TC7	50	403.437
TC8	75	272.911
TC9	100	186.798
TC10	150	0
TC11	200	95.578
TC12	250	80.933
TC13	300	67.11

Figure 3.11. Maximum temperature of each thermocouple in mix 5A..

Thermocouples	distance(mm)	Temperature max
TC1	1	987.453
TC2	5	250.09
TC3	10	908.456
TC4	15	1319.456
TC5	20	788.464
TC6	25	641.285
TC7	50	365.206
TC8	75	230.393
TC9	100	
TC10	150	
TC11	200	
TC12	250	41.732
TC13	300	32.923

	timbrok	tempbroke	relevant
broke	1.61	197.016	yes

Figure 3.12. Maximum temperature of each thermocouple in mix 5B..

Thermocouples	distance(mm)	Temperature max
TC1	1	1083.521
TC2	5	1086.118
TC3	10	987.026
TC4	15	999.186
TC5	20	900.411
TC6	25	785.686
TC7	50	520.277
TC8	75	326.281
TC9	100	199.187
TC10	150	116.8
TC11	200	98.595
TC12	250	80.404
TC13	300	68.688

	time broke	tembroke	relevant
broke	131.7492167	270.753	no
broke	126.6349	1031.978	no
broke	137.83885	284.155	no
broke	142.2678667	180.394	no
broke	180.4802833	313.944	no
broke	145.33	507.312	no

Figure 3.13. Maximum temperature of each thermocouple in mix 6A..

Thermocouples	distance(mm)	Temperature max
TC1	1	1371.567
TC2	5	1371.947
TC3	10	0
TC4	15	0
TC5	20	0
TC6	25	0
TC7	50	455.526
TC8	75	260.567
TC9	100	210.831
TC10	150	124.813
TC11	200	97.399
TC12	250	78.903
TC13	300	70.071

Figure 3.14. Maximum temperature of each thermocouple in mix 6B..

4

Compression and Tension Testing

"Work until your idols become your rivals" Drake

.

4.1. Compression and Tension Testing

Once performed the visual analysis of the cores we proceeded to slice each core into 3 parts. The piece exposed to the highest heat value, which acquired the yellowish color, was thrown away because all its mechanical properties were lost. The middle part is approximately from 100mm to 200mm. The back is from 200 mm to 300 mm. Knowing that 5mm of the back from the back piece was cut to assure a flat surface for the following compression tests. From each of the 5 cores from each block we now have 2 test samples called x (the one at the back, not exposed directly to the heat) and y (the middle part, closer to the heat but with useful mechanical properties).

From Figure 3.2 the samples in positions 1, 2 and 3 were submitted to compression testing. Cores 4 and 5 were rehearsed in tension.

Figure 4.1. Lawyers extracted from each core.

4.2. Compression

The aim of this test is to determine the variation of compression strength from the original concrete to the one exposed to the fire, by measuring strain, stress and deformation. Each sample was weighed, measured the height, top diameter, bottom diameter to determine the density, and the correction factor needed in each case. The standardization points out that a cylinder of 6 inch x 12 inch (150mm x300 mm) or 4 inch x 8 inch (100mm x 200mm), double the height than the base, should be used to do this tests. Unfortunately, samples of the same height and base (more specifically 100mm height and 94.6 diameter) were obtained. That is why a correction factor had to be used to get the real compresive strength which is shown in the table 4.2

L/D Ratio	Factor
1-1.02	0.87
1.03-1.06	0.88
1.07-1.1	0.89
1.11-1.15	0.9
1.16-1.19	0.91
1.2-1.23	0.92
1.24-1.29	0.93
1.3-1.38	0.94
0.39-1.46	0.95
1.47-1.56	0.96
1.57-1.69	0.97
1.7-1.81	0.98
1.82-1.94	0.99
1.95-2	1

Figure 4.2. Correction factor depending on the L/D relation..

The conclusions reached are the following:

- The back of mixes 1 and 4, non-fiber, can take up to 50 Mpa. The middle 45Mpa.
- The back of mix 2, including BarChips, can take 45 Mpa. The middle from 32Mpa to 42Mpa.
- The back of mix 3, BarChip plus Micro Polypropilene, can take up to 46 Mpa. The middle from 31 to 45Mpa.
- The back of mix 5, including Micro Polypropilene, can take from 35 to 41 Mpa. The middle from 30 to 40Mpa.
- The back of mix 6, including Micro Polypropilene and steel fibers, can take up to 50 Mpa. The middle 45 Mpa. This is very curious because the part closer to the heat resists better. This might be due to the steel fibers.

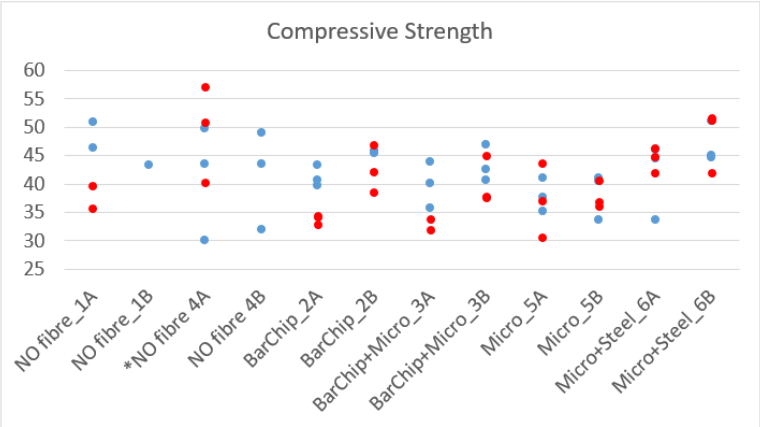

Figure 4.3. Plot of the compression strength for the back (blue) and middle (red) lawyers..

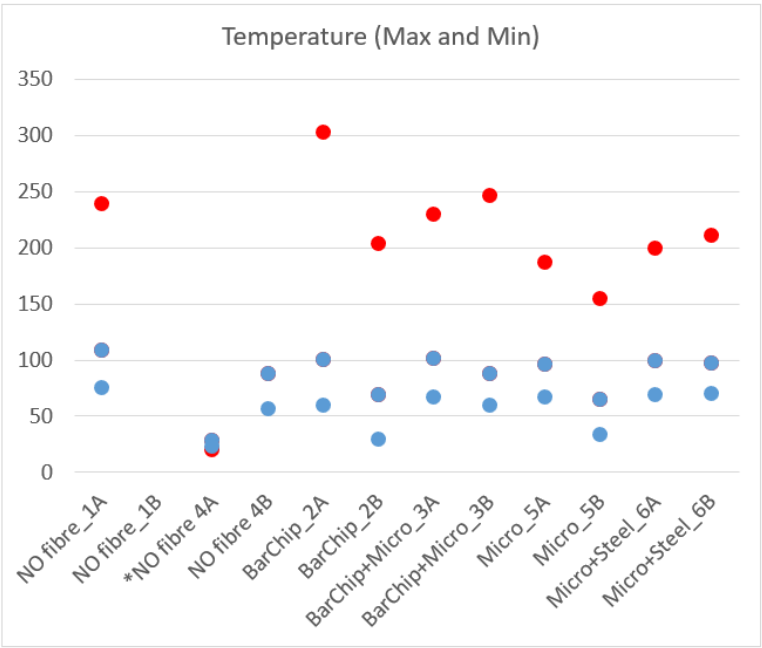

Figure 4.4. Plot of the Max (red) and min (blue) temperatures of each sample..

4.3. Tension

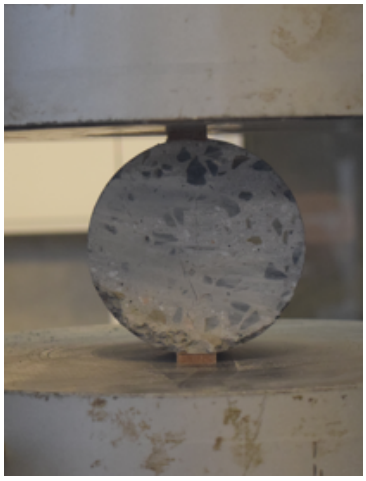

Figure 4.5. Example of a Brazilian test from one of the samples.

For the determination of the tensile strength the Brazilian test was performed. This is an indirect method for determining the tensile strength of a concrete material. The test requires the use of two hardboard bearing strips, nominally 5mm thick, 25 mm wide and at least as long as the specimen. Since the sample used was smaller than the standard, the width of the strips had to be modified.

$$\frac{150mm}{25mm} = \frac{94.6mm}{x}\ x = 15.8mm$$

Being 150 mm the diameter of the standard specimen and 94.6 the diameter of all the samples tested the width of both bearing strips was approximately 16mm. The length of these was 110, a little larger than the samples. The procedure for testing is as follows:

1. The bearing strips have to be placed between the top and bottom platen of the specimen.

2. Centering the specimen in the middle of the testing machine.

3. Apply a small initial force removing any side constrain.

4. Tare the machine and start the test by applying

$$1.5 \pm 0.15MPa \setminus min$$

   until no more can be sustained.

This ratio has to be modified to fit the machine (L is the length in mm, D is the diameter in mm)

Once the Test gives us the kN that each sample supports we have to correct it introducing the value in the equation (being P the maximum force applied indicated in the testing machine in KN; T is the indirect tensile strength in MPa):

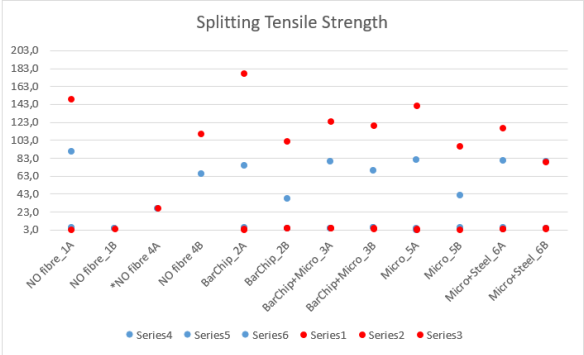

Figure 4.6. Plot of the tensile strength for the back (blue) and middle (red) layers.

5

Finite Element Simulations

"The harder you work for something the greater you will feel when you achieve it".

The first attempt at a numerical model was with the use of the software ansys. This chapter describes the procedure as well as the results obtained with this software. The highlight of the chapter is the explanation of the reasons why the tool was not ideal for the simulation of spalling.

5.1. Introduction

Ansys is a Finite Element Simulation tool with the main purpose of simulating how an specific model reacts under real conditions. It gives the user the ability to analyze a sample with a mesh meaning the sample can be studied to its deepest, the size of the mesh can be defined by the user depending on the precision needed. This project uses the thermal and structural tools within the software. To be specific the transient Thermal and Static structural were used.

5.2. Thermal Model

To be able to accomplish a thermal simulation the definition of certain parameters had to be established:

- Geometry of the sample: a 2D model was used sized 300x600 mm to simulate one layer of what was tested in The University of Queensland.
- Mesh size: to specify the nodes to be studied; the smaller the mesh the bigger the data sample. Starting with a smaller mesh to ensure its proper functionality.

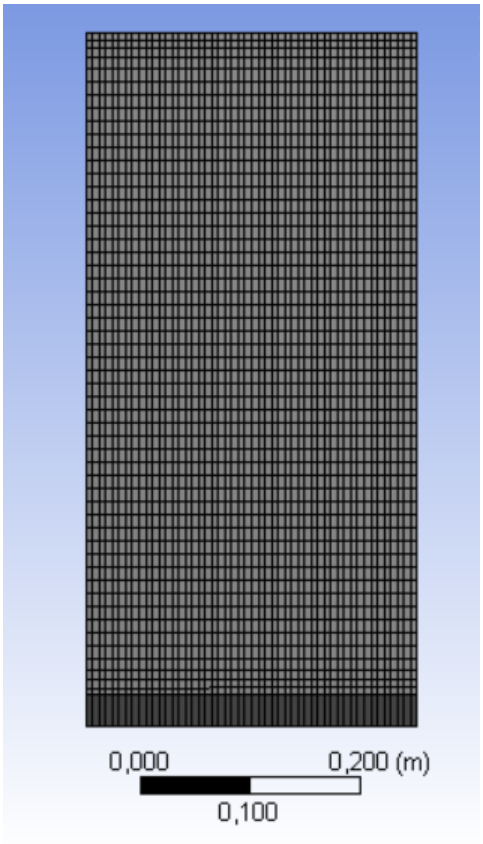

Figure 5.1. Mesh developed for the Ansys model.

- Material properties: following Eurocode and as determined in Chapter 2 Section 2.2. Density, Young's Modulus, Poisson's Ratio, Bulk Modulus, Shear Modulus, Isotropic Thermal Conductivity, Specific Heat, Compressive and Tensile Strength.
- Boundary conditions
  - Ambient temperature: set to 20 degrees Celsius.
  - Convection: a 25 W/m^2 C coefficient was set in three edges, top, left and right.
  - Radiation: with an emission of 0.4 applied in the top, left and right edge.
  - Adiabatic: the bottom of the sample was isolated when the real testing took place that is why we set an adiabatic boundary condition on the bottom of the sample.
  - Heat flux: heat flux applied on the right edge taking the data from the real experiment.

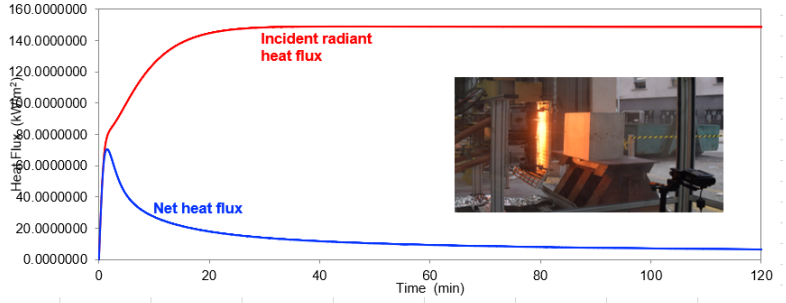

Figure 5.2. Heat flux data imported to the model from the experiment in The University of Queensland.

With all this input the simulation resulted on the data in the following images:

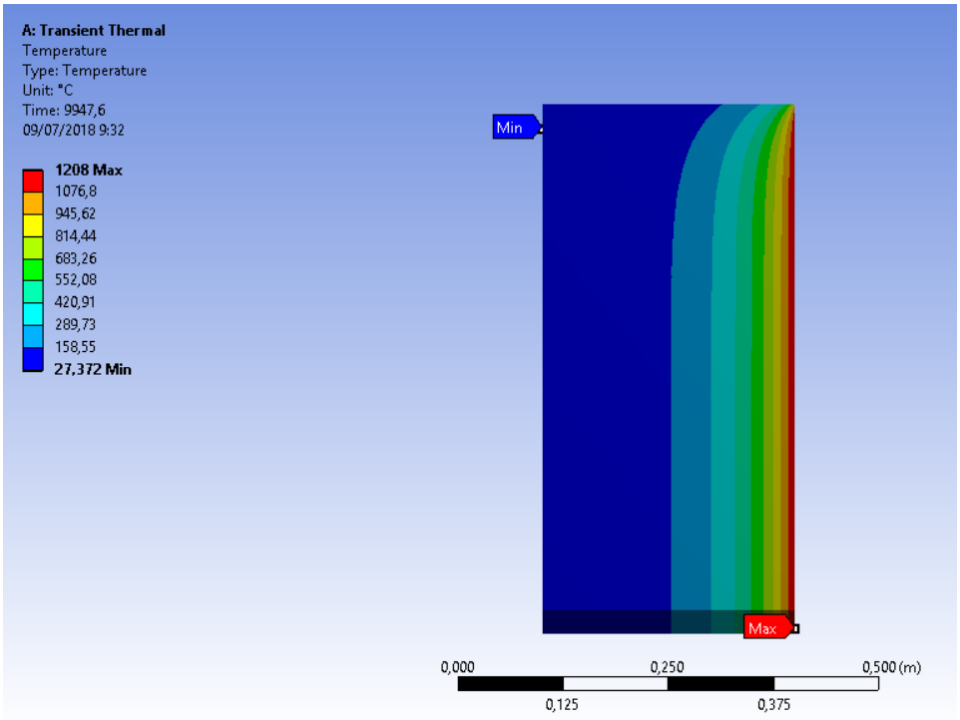

Figure 5.3. Temperature distribution resulting of the ansys simulation.

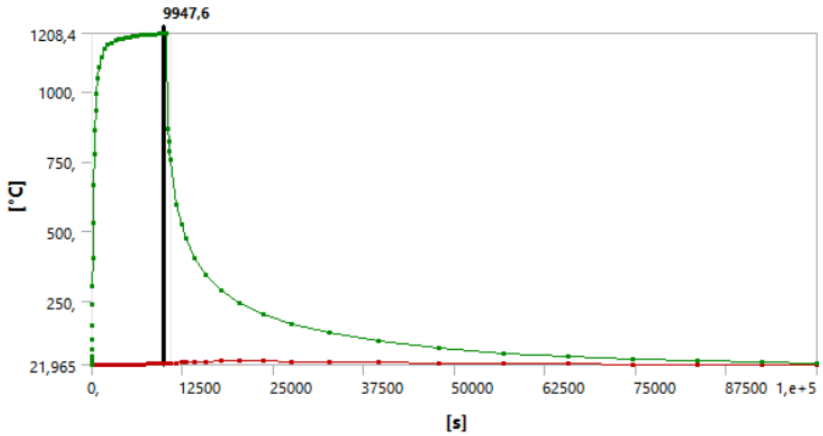

Figure 5.4. Temperature distribution through time graph resulting of the ansys simulation.

The data recorded with the thermo-couples of the batch tested of plain concrete had the following temperatures:

Thermocouples	Distance(mm)	Temperature max
TC1	1	1246.635
TC2	5	746.487
TC3	10	1014.597
TC4	15	1056.352
TC5	20	927.628
TC6	25	795.806
TC7	50	618.648
TC8	75	325.065
TC9	100	190.262
TC10	150	117.452
TC11	200	88.815
TC12	250	55.611
TC13	300	41.92
Exterior		28.395

Figure 5.5. Recorded temperature in the thermo-couples of plain concrete when exposed to the heat flux.

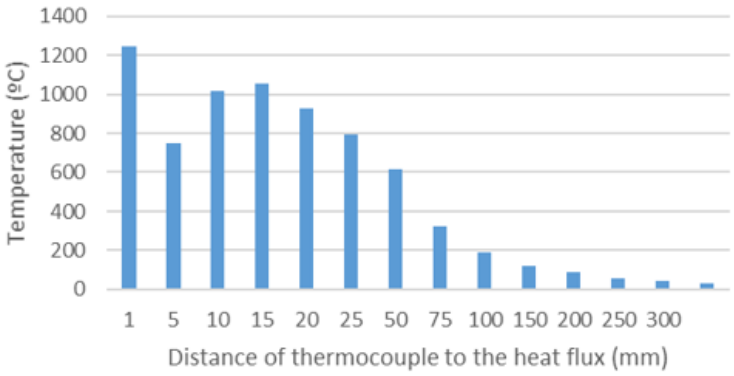

Figure 5.6. Graph of the recorded temperature in the thermo-couples of plain concrete when exposed to the heat flux.

The comparison shows considering each thermo-coupe. The first thermo-couple at 1 mm of the exposed surface read 1246^0C and 1208^0C in the simulation, which can be considered accurate. At 150 mm of the exposed surface the thermo-couple reads 117^0C and the simulation 150^0C. At the exterior the thermo-couple reads 42^0C and the simulation 27^0C. Overall, the model obtained was accurate for plain concrete. Ansys is a very useful and powerful tool yet the tool used for porous media (cpt212) has not been developed enough to simulate spalling. Moreover, moisture and drying phenomenons could not be simulated inside the tool.

5.3. Conclusions

Many parameters influence the appearance of the spalling effect but the main three are:

- Moisture
- Porous media
- Temperature

Ansys, does not consider moisture and the porous media tools are not developed enough for a project with these characteristics. Hence, it was decided that the tools was not strong enough and would not help with the development of the project.

Despite all these, the results obtained would be used for further comparison during the development of the ansys code through out the early stages when pores and moisture is not being considered because of the need to verify a less complex model.

6

Numerical Model with Matlab

"People cry not because they are weak but because they have been strong for too long." Jonnhy Depp

---

This chapter reproduces the numerical model which has been developed to gain a better understanding of the spalling phenomenon.

6.1. Introduction

Despite of Chapter 5 not giving a solution for our problem it was good to establish the following goals which helped give a deeper insight into the project and the real need and outcomes of it.

Ansys was our first software option due to the facilities it gives when it comes to introducing the geometry, the material properties, the boundary conditions. It is a very interactive and intuitive software with many functions that help the user introduce characteristics and also the lack of code makes it easier. Yet for our cause it was not powerful enough and another software had to be used.

Matlab will enable us to create our own model from scratch. This means that no original code is being used meaning that, in the long term, it will be easier to modify and insert new parameters: larger mesh, adding boundary conditions; different geometry.

All this will be achieved by the use of a PDE model. Firstly, a simple PDE model will be writen so as to compare the results with the data obtained in Ansys. After this has been achieved we will move on to the development of a more complex model with larger equations, temperature dependent boundary conditions and many other parameters that the researcher believes are necessary.

6.2. Reproducing plain concrete

Before inserting any complexity in the model with the addition of fibers it was necessary to understand how plain concrete behaves and to assure that it matched the experimental data obtained in the laboratory. A 2 dimensional geometry was created sized 300x600 mm. The main objective was to simulate the fire induced concrete and obtain the damaged material properties after the fire for a later discretion of nodes based on high temperature and stress in the material. When the limit values were reached the nodes where eliminated since the probability of spalling or the useless of the material are high.

This will result in a model which will give you the volume of the useful material after a fire.

6.2.1. PDE Model

The first step of the process was to define the type of model used. It was appropriate to use a PDE model (partial differential equations) due to the transient heat transfer equation being the one governing our model.

$$\rho Cp\frac{\partial T}{\partial t} = \frac{\partial}{\partial x}(k\frac{\partial T}{\partial x})$$

Being:

- ρ: density
- Cp: specific heat
- k: thermal conductivity

A PDE model lets you work with the number of equations, geometry, mesh and boundary conditions.

6.2.1.1. Geometry

The geometry defined is a 2D with dimensions 300 mm x 600 mm to get a close approach to the original materials rehearsed, (the original material was sized 300 x 600 x 500).

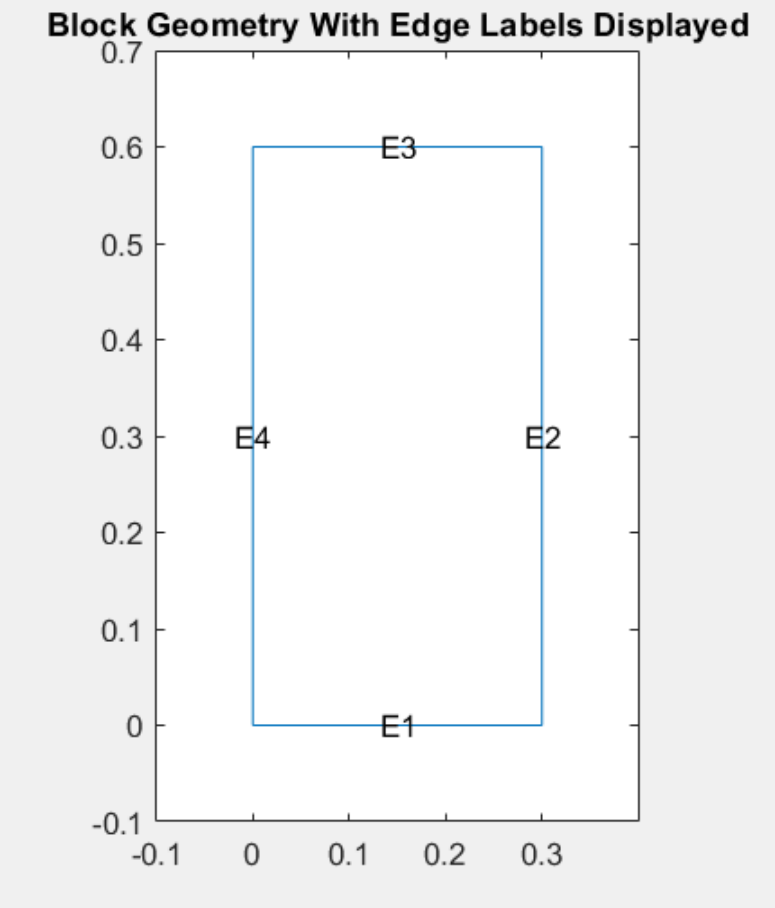

Figure 6.1. Geometry to be studied.

6.2.1.2. Mesh

The mesh generated had an element size of maximum 0.1.

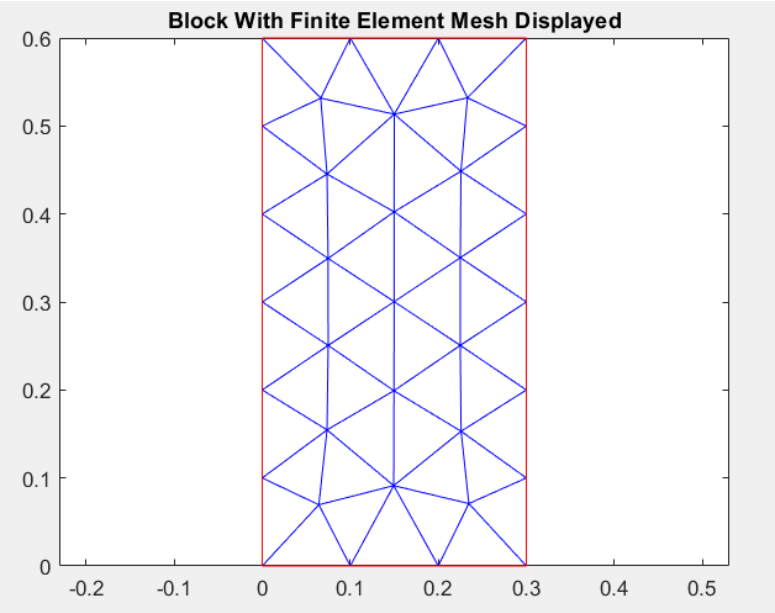

Figure 6.2. Mesh created.

6.2.1.3. Boundary Conditions

In this subsection the boundary conditions are going to be determined. First of all the heat flux should be inserted as a neumann boundary condition due to the heat flux being a derivative. Since the data obtained in the experiment provided us the heat flux as q but also as a temperature variable this data is set as a dirichlet boundary condition (differential equation).

This flux was inserted on the side of the geometry, as shown in Section 6.2.1.1) as side E4. The data is Figure 6.3.

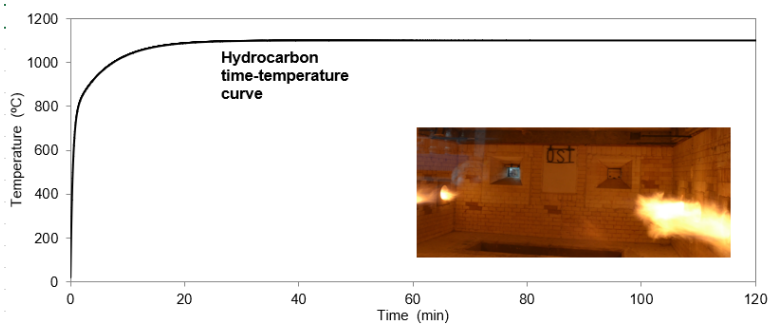

Figure 6.3. Temperature obtained by the heat flux generated in The University of Queensland.

Following the equation, which follows a dirichlet:

$$-k\frac{\partial T}{\partial x}\mid_{x=0}= q^s$$

Another boundary condition is the bottom of the sample which was isolated from any heat exposure, there for an adiabatic edge was established, following a neumann type of PDE equation:

$$\frac{\partial T}{\partial x}\mid_{x=0}= 0$$

The convection coefficient was set in all the faces excepting the bottom which, as said before, was isolated with adiabatic conditions. As well as this surface the convention follows neumann type of equation:

$$-k\frac{\partial T}{\partial x}\mid_{x=0}= h\left[T_{(infty)} - T(0,t)\right]$$

The last boundary condition is the constant ambient temperature of 20 ºC.

$$T(0,t) = T_s$$

These boundary conditions are introduced in the model with the tool "specifycoefficients".

$$m\frac{\partial^2 u}{\partial t^2} + d\frac{\partial u}{\partial t} - \bigtriangledown(c \bigtriangledown u) + au = f$$

This equation is the one given by matlab, our job was to introduce the parameters corresponding with the different equations used. The following subsections will specify these parameters (m,d,c,a,f) in correspondence with the pde model used.

6.2.2. Thermal model verification

The first step of the project was to build a simple code which could guarantee its functionality. This was done with a one equation PDE model and the constant coefficients set to the value 1. A unique boundary condition was set with a linear curve.
The equation resulted:

- m= 0
- d= ρ*Cp
- c= k
- a=0
- f=0

The code for these model can be found in Section 8.1.

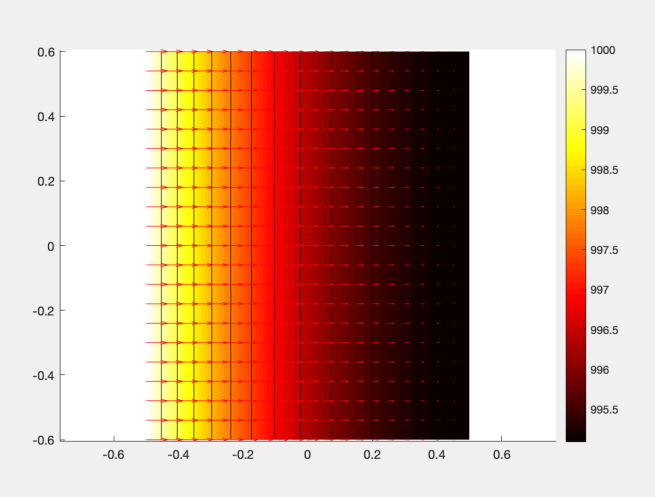

Figure 6.4. Matlab results for a transient Thermal with constant coefficients, heat flux.

This model worked perfectly and the results were logical so it was proceeded to non constant coefficients and the lower face with adiabatic conditions as well as the others with convection.

6.2.3. Transient Thermal

Once the simplest code worked, the code had to develop to a more precise and accurate program. The next step was to introduce non constant coefficients for the density, Cp, k. These values correspond to the Eurocode depending on the temperature of the material.
Once the non-constant boundary conditions worked the next step was to introduce the real heat flux curve.

The code for these model can be found in Section 8.2.

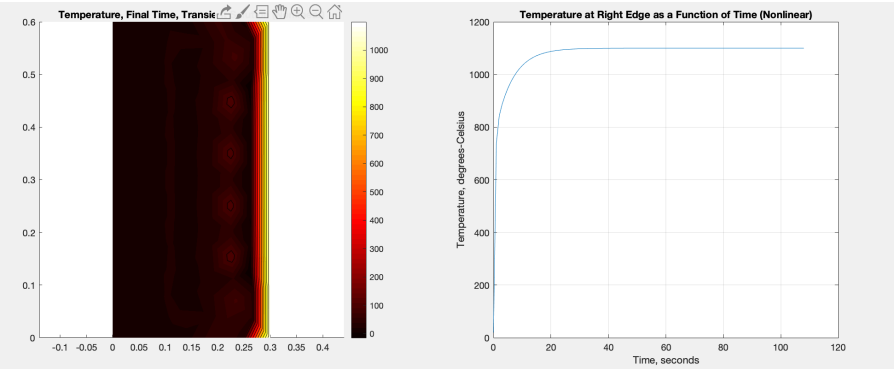

Figure 6.5. Matlab results for a transient Thermal .

As this complex model resulted in a success due to its comparison with the real heat curve obtained in The university of Queensland structural laboratory. The next step was to develop an independent moisture PDE model. So as to make sure it work for further fusion of both equations.

6.2.4. Moisture

As a complex thermal functioned perfectly. The code for moisture had to be written. The equation used was the following:

$$\frac{\partial M}{\partial t} = D\frac{\partial^2 M}{\partial x^2} + D\delta\frac{\partial^2 T}{\partial x^2} + W$$

Being:

- D= moisture diffusion coefficient.
- δ= thermal gradient coefficient
- W= moisture sink in concrete

The code for these model can be found in Section 8.3.

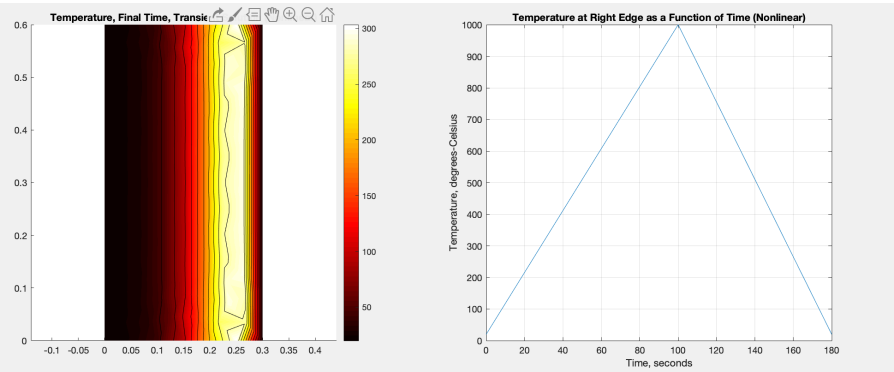

Figure 6.6. Matlab results for a transitient Thermal .

6.2.5. Thermal with moisture disengaged

After both codes operated correctly, the most challenging part of the thesis was the union of both codes in a 2 PDE model.

The complexity resided in the ability to integrate both codes. Which was not a simple task. The temperature dependent boundary conditions were achieved in this Matlab software with the use of a handle function. Unfortunately, as these type of functions did work in a PDE model with one equation, when using a matrix to introduce two (or more, in future work) equations another mechanism for temperature dependent variables has to be used.

$$\begin{bmatrix} \rho * Cp\frac{\partial}{\partial t} - \lambda\frac{\partial^2}{\partial x^2} & -\rho r h\frac{\partial}{\partial t} \\ -D\delta\frac{\partial^2}{\partial x^2} & \frac{\partial}{\partial t} - D\frac{\partial^2}{\partial x^2} \end{bmatrix} \begin{bmatrix} T \\ M \end{bmatrix} = \begin{bmatrix} Q \\ W \end{bmatrix}$$

Firstly, it was established to write a code which integrated both equations but at the same time these two were not engaged.

- m= 0
- d= [ρ*Cp 0 ρ*Cp 1]
- c= [k;0;k;k;0;k]
- a=[0;0]
- f=[0;0]

The code for these model can be found inSection 8.4.

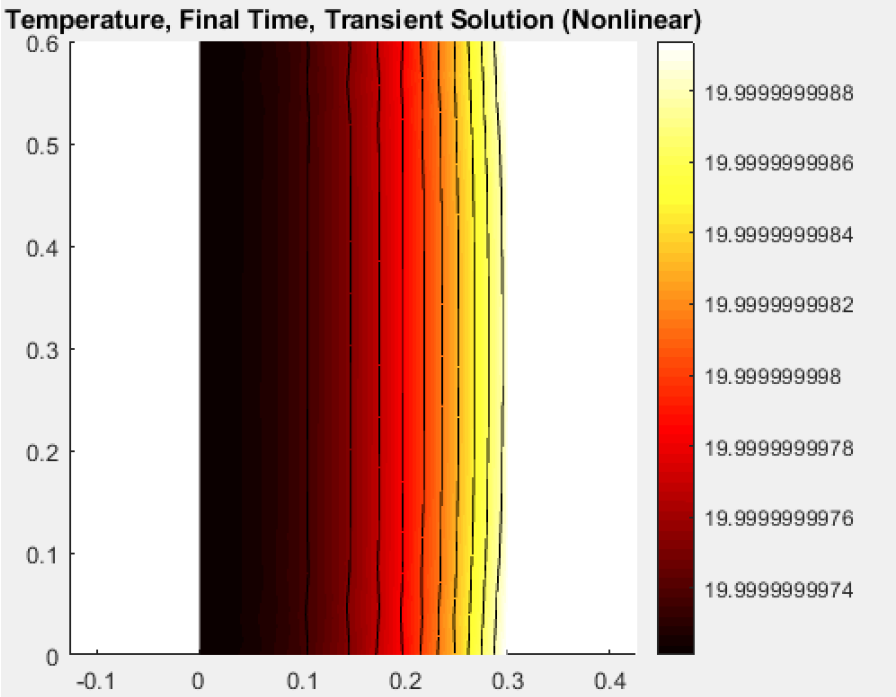

Figure 6.7. Matlab results for a 2 PDE model with a unique boundary condition.

With the application of the convection, the result was:

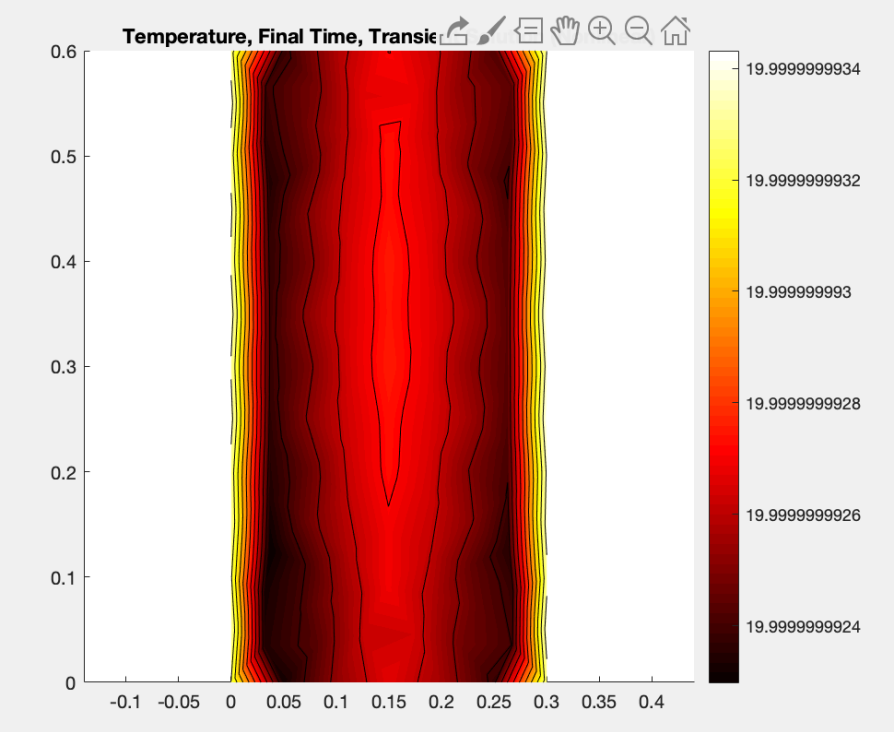

Figure 6.8. Matlab results for a 2 PDE model with a 3 boundary condition .

As this resulted in a success, the next step was to introduce the heat flux, as it is the most important boundary condition.
As mentioned before, for the three codes in the beginning handle functions were the solution to the non-constant boundary conditions. Yet when a more complex PDE model was written, with two equations (moisture and temperature) matrix were introduce to handle all the data. This matrices do not support handle functions.
Many attempts were made but no answer was found. The need of further research is needed.

6.2.6. Conclusion

After the use of Ansys software it was believed that Matlab would solve the problems reached in the previous software. This believe was shown to be true. Matlab helped with the thesis, it helped develop the whole project from the beginning and helped with the integration of all the parameters.

The project developed from a non existent work to a code which provides the user information for the analysis of the spalling effect.

7
Conclusion

This thesis had three main objectives:

- The experimentation in The University of Queensland: the exposure of concrete samples to heat flux; the analysis of these specimens (visual, compression, tension, thermal) and the study of the data obtained.
- Gather all the information in spalling and all the consequences as to know how each parameter influence the others so researchers could find a good source of information when needed.
- Develop a numerical program with the ability to simulate spalling.

The first and second objective, after many researches, many gathering of information, it was completed.

The third objective, with the use of different software's like Ansys and Matlab analyzing the pros and cons of both. Ansys, is an interactive and powerful software. It helps the user by offering a wide range of tools depending on the problem posed. In our case, concrete is a porous media, Ansys does have a tool (cpt212) for this kind of material yet it is not fully developed and no-one seems to have used it. Also the lack of utensils to introduce moisture in the material was enough to decide to move to another software which could help us with this matter. As spallings most important parameter is moisture, due to the water evaporating and moving through the pores, this determines how the crack is going to happen.

The lack of solution obtained with Ansys was not a failure. The results obtained would guarantee an appropriate comparison with the fist Matlab model produced as it did not contain moisture.

Matlab was the ideal tool for the project. Due to the ability to create our code from the beginning. At first a simple model was created, all the difficulties were put behind and step by step a more complex model was created.

When it came to the fusion of the moisture and thermal equation, many developments, many trial and errors were needed but when the heat flux had to be introduce the lack of time did not allow us to finish the simulation. Many attempts were made for the solution of a two PDE model, yet this could not be acquired and the project had to come to and end.

7.0.1. Future

When this project was accepted it was known to be quite challenging because as many researches have tried to simulate spalling no-one has managed to obtain accurate results. That is another reason why the development of a code from the beginning was a good idea.

This project can be the beginning of further researches. It is believed that much progress was made through out the two years working on it and this will help further students or researches with the full development of the entire code to simulate spalling.

8

Annex

In this chapter we can find the code developed for all parts of the project.

8.1. Thermal Model Verification Code

```
% Create a PDE Model with a single dependent variable
pdem = createpde();
% Geometry
r1 = [3 4 -.5 .5 .5 -.5 -.6 -.6 .6 .6];
gdm = [r1]';
g = decsg(gdm,'R1',['R1']');


    % Convert the decsg format into a geometry object
geometryFromEdges(pdem,g);
figure pdegplot(pdem,'EdgeLabels','on');
axis([-.9 .9 -.9 .9]);
title 'Block Geometry With Edge Labels Displayed'


    % PDE Coefficients and Boundary Conditions
uLeft = applyBoundaryCondition(pdem,'dirichlet','Edge',4,'u',@temptime3);


    % Coefficient Definition
rho =1; % density
Cp = 1; % specific heat
k =1; % thermal conductivity


    c = k;
a = 0;
f = 0;
d = rho.*Cp;
specify Coefficients(pdem,'m',0,'d',d,'c',c,'a',a,'f',f);


    % Mesh hmax = .1; % element size
msh=generateMesh(pdem,'Hmax',hmax);
figure
pdeplot(pdem);
axis equal
title 'Block With Finite Element Mesh Displayed'


    % Transient Solution
tlist = 0:.5:100;
setInitialConditions(pdem, 20);
results = solvepde(pdem,tlist);
u = results.NodalSolution;


    %Graph
```

```
    cgradx,cgrady
= evaluateCGradient(results);
pdeplot(pdem,'XYData',u(:,end),'Contour','on','FlowData',[-cgradx(:,end),-cgrady(:,end)],'ColorMap','hot')


    getClosestNode = @(p,x,y) min((p(1,:) - x).^2 + (p(2,:) - y).^2);


    h = figure
; h.Position = [1 1 2 1].*h.Position;
subplot(1,2,1);
axis equal pdeplot(pdem,'XYData',u(:,end),'Contour','on','ColorMap','hot');
axis equal
title 'Temperature, Final Time, Transient Solution (Nonlinear)' subplot(1,2,2);
axis equal plot(tlist(1:size(u,2)), u(nid,:));
grid on
title 'Temperature at Right Edge as a Function of Time (Nonlinear)';
xlabel 'Time, seconds'
ylabel 'Temperature, degrees-Celsius'
```

8.2. Transitient thermal Code

```
% Create a PDE Model with a single dependent variable
pdem = createpde();
% Geometry
r1 = [3 4 0 .3 .3 0 0 0 .6 .6];
gdm = [r1]';
g = decsg(gdm,'R1',['R1']');


    % Convert the decsg format into a geometry object
geometryFromEdges(pdem,g);
figure pdegplot(pdem,'EdgeLabels','on');
axis([-.1 .4 -.1 .7]);
title 'Block Geometry With Edge Labels Displayed'
h = @(loc,state) 25*(20-(state.u));
% PDE Coefficients and Boundary Conditions
uBottom = applyBoundaryCondition(pdem,'neumann','Edge',1,'g',0);
%Adiabatico uc3 = applyBoundaryCondition(pdem,'neumann','Edge',3,'g',h);
uc4 = applyBoundaryCondition(pdem,'neumann','Edge',4,'g',h);
uc2 = applyBoundaryCondition(pdem,'neumann','Edge',2,'g',h);
uLeft = applyBoundaryCondition(pdem,'dirichlet','Edge',2,'u',@temptime2);
k = @(loc,state) 1+10.^(-6)*(state.u).^2-0.0024*(state.u)+1.9538;
t = @(loc,state)-0.000000036*(state.u).^4+.000195213*(state.u).^3-1.0887216*(state.u).^2+
1036.7035*(state.u)+2170505.4;
c = k;
a = 0;
f = 0;
d = t;
specifyCoefficients(pdem,'m',0,'d',d,'c',c,'a',a,'f',f);


    % Mesh
hmax = .1;
% element size
msh=generateMesh(pdem,'Hmax',hmax);
figure
pdeplot(pdem);
axis equal
title 'Block With Finite Element Mesh Displayed'


    % Transient Solution
tlist = 0:1:108;
setInitialConditions(pdem, 20);
results = solvepde(pdem,tlist);
u = results.NodalSolution;
```

```
    getClosestNode = @(p,x,y) min((p(1,:) - x).^2 + (p(2,:) - y).^2);
% Call this function to get a node near the center of the right edge. [ ,nid] = getClosestNode(
msh.Nodes, .5, 0 );


    h = figure;
h.Position = [1 1 2 1].*h.Position; subplot(1,2,1);
axis equal pdeplot(pdem,'XYData',u(:,end),'Contour','on','ColorMap','hot');
axis equal
title 'Temperature, Final Time, Transient Solution (Nonlinear)' subplot(1,2,2);
axis equal plot(tlist(1:size(u,2)), u(nid,:));
grid on
title 'Temperature at Right Edge as a Function of Time (Nonlinear)';
xlabel 'Time, seconds'
ylabel 'Temperature, degrees-Celsius'
```

8.3. Moisture Code

```
% Create a PDE Model with a single dependent variable
moist = createpde();
% Geometry
r1 = [3 4 0 .3 .3 0 0 0 .6 .6];
gdm = [r1]';
g = decsg(gdm,'R1',['R1']');


    % Convert the decsg format into a geometry object geometryFromEdges(moist,g);
figure pdegplot(moist,'EdgeLabels','on'); axis([-.1 .4 -.1 .7]);
title 'Block Geometry With Edge Labels Displayed' h = @(loc,state) 25*(20-(state.u));


    uLeft = applyBoundaryCondition(moist,'dirichlet','Edge',2,'u',@temptime3);


    % Coefficient Definition
cc = 0.0000282;
dd = 1;
specifycoefficients(moist,'m',0,'d',dd,'c',cc,'a',0,'f',0);


    % Mesh
hmax = .1;
% element size
msh=generateMesh(moist,'Hmax',hmax);
figure
pdeplot(moist);
axis equal
title 'Block With Finite Element Mesh Displayed'


    % Transient Solution
tlist = 0:1:180;
setInitialConditions(moist, 20);
results = solvepde(moist,tlist);
u = results.NodalSolution;


    [ ,nid] = getClosestNode( msh.Nodes, .5, 0 );


    h = figure;
h.Position = [1 1 2 1].*h.Position;
subplot(1,2,1);
axis equal pdeplot(moist,'XYData',u(:,end),'Contour','on','ColorMap','hot');
axis equal
title 'Temperature, Final Time, Transient Solution (Nonlinear)' subplot(1,2,2);
axis equal plot(tlist(1:size(u,2)), u(nid,:));
```

```
grid on
title 'Temperature at Right Edge as a Function of Time (Nonlinear)';
xlabel 'Time, seconds'
ylabel 'Temperature, degrees-Celsius'
```

8.4. Thermal with moisture disengaged Code

```
% Create a PDE Model with a single dependent variable numberOfPDE = 2;
pdem = createpde(numberOfPDE);


    % Geometry
r1 = [3 4 0 .3 .3 0 0 0 .6 .6];
gdm = [r1]';
g = decsg(gdm,'R1',['R1']');


    % Convert the decsg format into a geometry object
geometryFromEdges(pdem,g);
figure pdegplot(pdem,'EdgeLabels','on'); axis([-.1 .4 -.1 .7]);
title 'Block Geometry With Edge Labels Displayed' h = @(loc,state) 25*(20-(state.u));
hh = 10;
% PDE Coefficients and Boundary Conditions
uBottom = applyBoundaryCondition(pdem,'neumann','Edge',1,'g',[0,0]); %Adiabatico
%uc3 = applyBoundaryCondition(pdem,'neumann','Edge',[3,4],'g',[h,hh]);
uc4 = applyBoundaryCondition(pdem,'neumann','Edge',4,'g',h);
uc2 = applyBoundaryCondition(pdem,âneumann','Edge',2,'g',h);
%uLeft = applyBoundaryCondition(pdem,'dirichlet','Edge',2,'u',[@temptime3,0]);
k = 1.5;
t = 2400*1000;
c= [k;0;k;k;0;k]; a = [0;0];
f= [0;0];
d = [t 0 t 1]';
m = 0 specifyCoeï¬¬cients(pdem,' m', m,' d', d,' c', c,' a', a,' f', f);
% Mesh hmax = .1; % element size
msh=generateMesh(pdem,'Hmax',hmax);
figure
pdeplot(pdem); axis equal
title 'Block With Finite Element Mesh Displayed
'


    % Transient Solution
tlist = 1:1:108;
u0 = [20;2];
ut0=[0;0];
% only if m was nonzero
setInitialConditions(pdem,u0,ut0); r
esults = solvepde(pdem,tlist);
u = results.NodalSolution;


    % Graph
getClosestNode = @(p,x,y) min((p(1,:) - x).^2 + (p(2,:) - y).^2);
% Call this function to get a node near the center of the right edge. [ ,nid] = getClosestNode(
msh.Nodes, .5, 0 );
```

```
h = figure;
h.Position = [1 1 2 1].*h.Position; subplot(1,2,1);
axis equal pdeplot(pdem,'XYData',u(:,end),'Contour','on','ColorMap','hot');
axis equal
title 'Temperature, Final Time, Transient Solution (Nonlinear)' subplot(1,2,2);
axis equal
% plot(tlist(1:size(u,2)), u(nid,:));
plot(tlist(:,abs(u)), u(nid,:));
grid on
title 'Temperature at Right Edge as a Function of Time (Nonlinear)';
xlabel 'Time, seconds'
ylabel 'Temperature, degrees-Celsius'
```

Bibliografía

Bibliography

[1] **Helmut Kupfer, Hubert K. Hisdorf, Hubert Rusch.**, *Behaviour of concrete under biaxial stresses*

[2] **Sing Yupu Zhang zhong, QING LIKUN, Yu Changjiang.**, *Biaxial tensile-compressive experiment of concrete at high temperatures* Spring-Summer 2017

[3] **BS EN 1992-1-2:2004**, *Eurocode* July 2008

[4] **Metin Husem.**, *The effects of high temperature on compressive and flexural strengths of ordinary and high-performance concrete* December 2005

[5] **Milos Vasic, Zeljko Grbavcic, Zagorka Radojevic**, *Determination of the moisture diffusivity coefficient and mathematical modeling of drying* December 2013

[6] **Xin Yu, Arthur R. Schimidt, Luis A. Bello-Perez, Shelly J. Schimidt**, *Determination of the Bulk Diffusion Coefficient for Corn Starch Using an Automated Water Sorption Instrument* December 2007

[7] **Thomas Gernay, Vlado Peric, Boyan Mihaylov, Tom Molkens, Jean-Mark Franssen**, *Effect of upgrading concrete strength class on fire performance of reinforced concrete columns.*

[8] **BRupali V. Dhanadhya, Abhay S.Nilawar, Yogesh L. Yenarkar.**, *Theoretical study and finite element analysis of convective heat transfer augmentation from horizontal rectangular fin with circular perforation* June 2013

[9] **Gyu-Yong Kim, Gyeong-Cheol Choe, Min-Ho Yoon, Eui-Chul Hwang**, *Effect of High Temperature Elastic Modulus on Thermal Strain Behaviour of Ultra High Strength Concrete* September 2016

[10] **Mohammad Hassan Baziar**, *International Journal of civil engineering* December 2010

[11] **Izabela Hager, Tomasz Zdeb**, *Influence of curing conditions on spalling behaviour of reactive powder concretes* October 2011

[12] **Professor Grabriel Alexander Khoury, Dr. Yngve Anderberg.**, *Concre Spalling Review* June 2000

[13] **Cristian H. Maluk Zedan.**, *Development and Application of a Novel Test Method for Studying the Fire BEhaviour of CFRP Prestressed Concrete Structural Elements.* 2014

[14] **I.J.J van Straalen, R.D.J.M. Steenbergen, S.S.K. Lentzen, R. de Vries..**, *Simplified stochastic modeling of concrete spalling due to fire.* 2013

[15] **The-Duong Nguyen, Fekri Meftah.**, *Behaviour of Hollow Clay Brick Masonry Walls during Fire. Finite Element Modeling and Spalling Assessment.* October 2013

[16] **Jie Zhao, Jian-Jun Zheng, Gai-Fei Peng, Klaas van Breugel.**, *Numerical Analysis of heating rate effect on spalling of high-performance concrete under High Temperature Conditions.* 2017

[17] **Venkatesh Kodur.**, *Properties of concrete at elevated temperatures.* March 2013

[18] **Shohana Iffat.**, *Relation Between Density and Compressive Strength of Hardened Concrete.* January 2016

[19] **5th International Workshop on Concrete Spalling.**, *Concrete Spalling due to fire Exposure.* October 2017

[20] **Ronald E.Benson Jr.,Benjamin L. Sill.**, *The use of integral methods in solving partial differential equations.*

[21] **Rohit Singh.**, *Validation of Pore Pressure Theory on Fire Spalling of Concrete.* May 2016

[22] **O. Bahr, P. Schaumann, B. Bollen, J. Bracke.**, *Young´s Modulus and Poisson´s ratio of concrete at high temperatures: Experimental investigations.* August 2012

[23] **Cristian H. Maluk Zedan.**, *Development and Application of a Novel Test Method for Studying the Fire BEhaviour of CFRP Prestressed Concrete Structural Elements.* 2014